Discover Oncology

Analysis

Comprehensive analysis of the prognosis and tumor immune microenvironment of ubiquitin-conjugating enzyme transport-related gene UBE2C in hepatocellular carcinoma

Yang Xu[1] · Fei Lan[1] · Qiang Bi[1] · Xinyi Li[1] · Zhiyu Wang[1] · Ying Li[1] · Pengfei Li[1] · Haichen Long[1] · Li Du[1]

Received: 30 December 2024 / Accepted: 12 May 2025
Published online: 23 May 2025

Abstract

Ubiquitin-conjugating enzyme E2 C (UBE2C) is involved in tumor progression and cellular processes in many cancers and is implicated in cell cycle regulation. However, its prognostic significance in Hepatocellular carcinoma (HCC) and the mechanism of tumor immune response are unknown. The expression of UBE2C genes in HCC and normal tissue samples was investigated based on The Cancer Genome Atlas (TCGA) LIHC dataset and validated by Gene Expression Omnibus and Human Protein Atlas. Subsequently, the relationship between UBE2C gene expression, clinicopathologic parameters, and each survival period was investigated by regression analysis and Kaplan-Meier survival curves. The set of genes co-expressed with UBE2C was constructed and subjected to genomic enrichment analysis, GO and KEGG pathway enrichment analysis. Finally, the relationship between UBE2C gene expression and immune cell infiltration, immunosuppressive molecules in tumor samples from the TCGA-LIHC dataset was investigated. UBE2C gene expression levels were significantly higher in HCC samples compared to normal samples ($p < 0.05$). Higher UBE2C gene expression was closely associated with higher tumor grade and later tumor stage. The results of Kaplan-Meier survival curves showed that the survival of HCC patients with high UBE2C expression was shorter than that of patients with low UBE2C expression ($p < 0.05$, HR(CI) = 1.870[1.276, 2.741]). The results of PPI showed a high correlation between cell cycle-related proteins and UBE2C gene expression. Additionally, the highly expressed UBE2C gene was associated with an increased number of immunosuppressive molecules. UBE2C is an independent predictive marker for HCC patients, and the prognostic value of survival is improved when combined with clinical stage information. This study reveals its potential as a prognostic biomarker and as a new target for HCC intervention.

Keywords UBE2C · Hepatocellular carcinoma · Tumor immune microenvironment · Prognosis · Biomarker

Yang Xu, Fei Lan and Haichen Long have contributed equally to this work and should be considered to this work and should be considered co-first authors.

Supplementary Information The online version contains supplementary material available at https://doi.org/10.1007/s12672-025-02675-0.

✉ Pengfei Li, Lipf282992@163.com; ✉ Haichen Long, 2216177915@qq.com; ✉ Li Du, 2290612710@qq.com | [1]College of Medicine, Tarim University, Alar 843300, Xinjiang, China.

1 Introduction

HCC is the most common form of liver cancer, accounting for about 90% of cases. The primary risk factors for developing hepatocellular carcinoma are infections caused by the Hepatitis B virus and Hepatitis C virus [1]. According to the 2020 data, hepatocellular carcinoma (HCC) has emerged as the third leading cause of cancer-related mortality on a global scale, with a persistent upward trajectory in its incidence [2]. The combination of molecularly targeted therapies and immunotherapies is emerging as a tool to enhance the immune system's response to HCC-derived neoantigens [3]. In this context, bioinformatics methods with the advantages of large sample sizes and high efficiency have been widely used in cancer research. This study aims to study cancer diagnosis, prognosis, and immunotherapy using publicly accessible databases.

Ubiquitin-conjugating Enzyme E2 C (UBE2C) plays a crucial role in the ubiquitin-proteasome system as a member of the ubiquitin-coupled enzyme complex. It has been shown that dysregulation of the ubiquitination process plays a vital role in the development and progression of cancer, making ubiquitination a new therapeutic target for the treatment of cancer [4, 5]. UBE2C is activated by initiating ubiquitination modifications of cell cycle-associated proteins to ensure normal progression [6]. Numerous studies have demonstrated that UBE2C has relatively low expression in normal tissues but presents high expression in tumor cells, such as colorectal [7], breast [8], lung [9], adrenocortical [10], thyroid [11], and hepatocellular carcinoma [12]. Previous studies confirmed that UBE2C is highly expressed in HCC and has a shorter survival, which portends a poor prognosis [13–16]. However, there are fewer studies on the relationship between UBE2C and HCC immune infiltration.

To elucidate the possible correlation between UBE2C and HCC, this study conducted an integrative analysis of UBE2C through cancer-related databases such as TCGA and GEO and delved into the relationship between UBE2C expression and various immune cell infiltration.

2 Materials and methods

2.1 Data sources

2.2 TCGA database and GTEx database

TCGA (https://portal.gdc.cancer.gov/) provides clinicopathologic data about 33 distinct cancer types. It serves as a publically accessible data platform for extensive cancer genome initiatives [17]. High-throughput RNA sequencing (RNA-Seq) information and clinical data by searching the TCGA database for ALL (pan-cancer) projects and TCGA-LIHC in level 3 HTSeq-FPKM format. TCGA-LIHC includes 374 tumor samples and 50 normal control samples. Log2 transformation of RNA-Seq data in FPKM format was used for subsequent R package analysis. As the database is publicly available, it does not require the approval of the local ethics committee. The GTEx database contains a large number of normal human tissue samples. RNA-Seq information in the liver was obtained from the GTEx database, which contains information on 110 normal samples [18].

2.3 GEO and HPA databases

The Gene Expression Omnibus (GEO, www.ncbi.nlm.nih.gov/geo/) is a globally accessible library with high-throughput microarray and next-generation sequence functional genomic data that the research community has contributed [19]. The study included the GSE121248 and GSE84402 datasets from the GEO database. The GSE121248 includes 37 normal and 70 tumor samples [20], and the GSE84402 includes 14 normal and 14 tumor samples [21].

The HPA contains a large amount of data on various human tissues, cells, pathology profiles, and proteomes [22]. In addition, the database offers comprehensive information regarding the immunohistochemistry measurements of proteins in both tumor and normal human tissue specimens. Immunohistochemical data of UBE2C differentially expressed proteins in HCC, and normal human tissues were retrieved from the HPA database.

2.4 Characterization of UBE2C gene expression

An analysis was conducted on the expression of UBE2C in different tumor tissues and adjacent normal tissues, utilizing many databases such as TIMER2.0 [23], TCGA, and GTEx. RNA-Seq data obtained from TCGA and GTEx were visualized

using R software version 4.3.3 and the "ggplot2" package. In the statistical analysis, $P < 0.05$ was considered statistically significant, and the P values were normalized using the Bonferroni method. In order to assess the distinguishing expression of UBE2C in hepatocellular carcinoma tissues and normal control tissues, an analysis was conducted using immunohistochemistry (IHC) pictures obtained from the Human Protein Atlas (HPA) of both tumor and normal tissues.

2.5 Prognostic role of genetic characterization

Prognostic parameters such as Disease-Specific Survival (DSS), Overall Survival (OS), Disease-Free Interval (DFI), and Progression-Free Interval (PFI) were analyzed using the "survival" package for TCGA patient data, and the thresholds for the high- and low-expression UBE2C groups were determined using 1/3 values. The Wilcoxon signed-rank sum test was used to determine the relationship between UBE2C expression and clinicopathologic features, and whether prognostic genetic features were independent of other clinical parameters was predicted by univariate and multivariate Cox regressions, with $p < 0.05$ considered statistically different. The probability of HCC 1-, 3-, and 5-OS was also predicted by constructing nomogram plots and comparing them with the actual incidence using calibration curves, with the 45-degree line indicating the most accurate predictive value.

2.6 Enrichment analysis

In order to investigate the biological function of UBE2C, the "limma" package was used to analyze the TCGA-LIHC dataset of patients with high and low expression of UBE2C, and a total of 106 co-expressed genes were identified with the screening criterion of $|\text{LogFC}| > 1.5$ and $p < 0.05$. The role of UBE2C in liver cancer was verified by Gene Ontology (GO) analysis. A total of 106 co-expressed genes were identified, and the role of UBE2C in hepatocellular carcinoma was verified by GO analysis, followed by Go Set Enrichment Analysis (GSEA) using the clusterPrifiler package to identify the enriched pathways. In addition, genes differentially expressed with UBE2C were imported into the STRING database [24, 25], the significance threshold was set at a confidence score greater than 0.4, the nodes not associated with the network were hidden, and its biological function was visualized by Cytoscape 3.10.2 and ClueGO plugin.

2.7 Analysis of somatic mutation

The mutation status of the high and low UBE2C expression groups was determined and mapped using the "maftools" package to obtain HCC SNV mutation data. Differences and similarities in mutation type, SNV classification, and mutation rate between the high and low UBE2C expression groups were evaluated, and the top 30 genes with the highest mutation rate were filtered out. Waterfall plots were also drawn to show the mutation status of the mutated genes.

2.8 Integrated analysis of the immune profile of different expression groups

Anti-tumour immunity can be conceptualized as a series of events including the release of cancer cell antigens (step 1), cancer antigen presentation (step 2), priming and activation (step 3), trafficking of immune cells to tumors (step 4), infiltration of immune cells into tumors (step 5), recognition of cancer cells by T cells (step 6), and killing of cancer cells (step 7) [26]. These processes reflect the tumor recognition and killing process and influence the outcome of tumor immunotherapy. To further compare whether there are differences in anti-tumor immunity between different UBE2C expression groups, gene sequences representing these seven steps of anti-tumor immunity were collected from the Tumour Immunophenotype Tracking (TIP) database [26]. Tumor characteristics of different UBE2C expression groups were assessed using seven immune process scores from the TIP database of antitumor immune cycles of HCC tumor specimens.

In addition, to further assess the differences in immune cell infiltration between different UBE2C expression groups. Tumor immune infiltration analysis was performed using the "GSVA" and "CIBERSORT" software packages, including 16 different types of immune cells and 13 immune function scores obtained from He et al. [27]. The strength of the association between UBE2C gene expression and different types of immune cell infiltration was then assessed by the Spearman correlation algorithm. The log2-transformed gene expression matrix was uploaded to the TIDE database (http://tide.dfci.harvard.edu/) [28] to assess the differentiation of tumor immune dysfunction and rejection (TIDE) scores. Estimated scores, immune scores, stromal scores, and tumor purity were calculated for each tumor sample in the TCGA-LIHC dataset using the "ESTIMATE" software package. In addition, the correlation between UBE2C expression and immunosuppression was analyzed using the TISIDB database [29].

3 Results

3.1 Differential expression of UBE2C

The flowchart of this study is shown in Fig. 1. High UBE2C expression is common in tumor tissues (Fig. 2A). This phenomenon was similarly verified by the TIMER2.0 database (Fig. 2B). In the TCGA-LIHC dataset, UBE2C expression was significantly elevated in HCC primary tumor samples ($p < 0.001$) (Fig. 2C). In addition, the expression of UBE2C was also compared in TCGA tumor samples and GTEx normal samples, and UBE2C was found to be significantly up-regulated in tumor tissues ($p < 0.001$) (Fig. 2D). Subsequently, a subjective operating characteristic (ROC) curve was constructed to determine the diagnostic significance of UBE2C expression. The results of the study showed an area under the curve (AUC) value of 0.978 (CI = 0.964–0.992), suggesting a solid diagnostic potential for UBE2C (Fig. 2E). In addition, UBE2C was significantly up-regulated in HCC samples compared to corresponding adjacent tissue samples ($p < 0.001$) (Fig. 2F). Furthermore, it was verified that UBE2C gene expression was significantly up-regulated in HCC using the GEO dataset (GSE121248, GSE84402) (Fig. 2G, H). The p-values were normalized for differential expression across data sets (Table 1). Finally, the relative expression of the UBE2C protein was compared using immunohistochemical data from the HPA database (Fig. 2I). The results showed that UBE2C protein was expressed more in tumor samples than in normal tissue samples, suggesting that the expression patterns of UBE2C protein and RNA were comparable in the database.

3.2 Relationship between UBE2C expression and clinical features

UBE2C expression differed from T-stage, pathologic stage, histologic grade, and OS event (death) ($P < 0.05$) (Fig. 3A–H). The accuracy of this result was verified according to the chi-square test (Table 2). In addition, studies using univariate methods showed that UBE2C expression correlated with other clinical characteristics, especially age (OR = 1.67 (1.09–2.55), $p = 0.018$), pathological stage (OR = 2.05 (1.25–3.36), $p = 0.004$) and histological grading (OR = 2.82

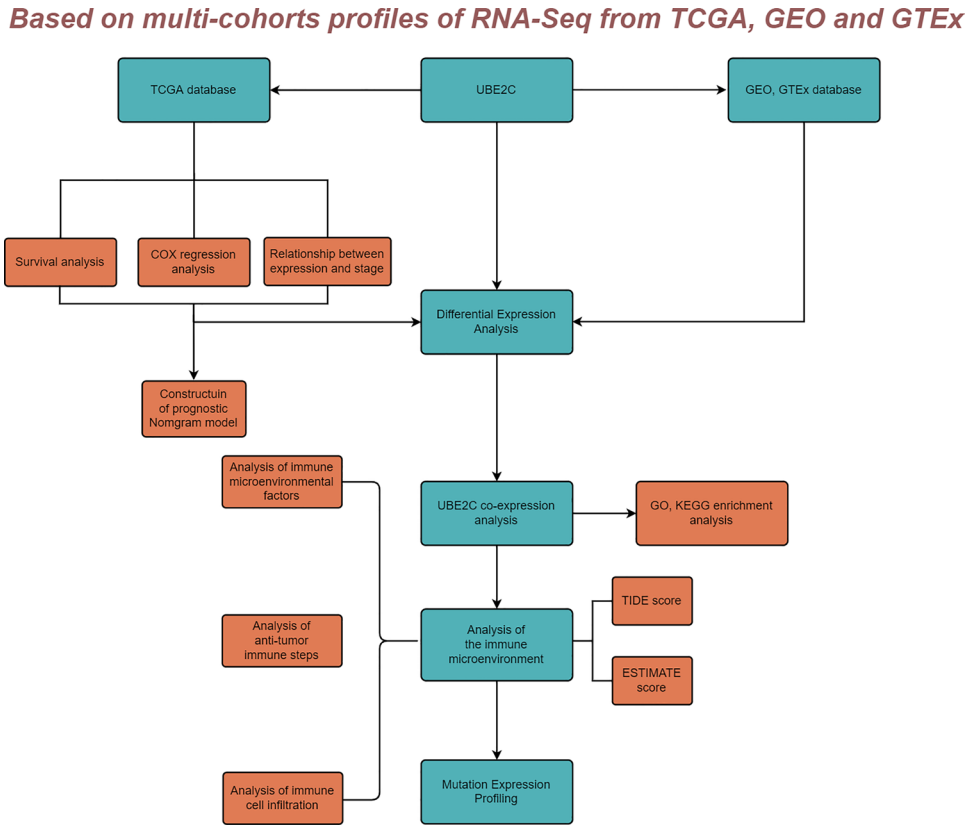

Fig. 1 The flowchart of the current study

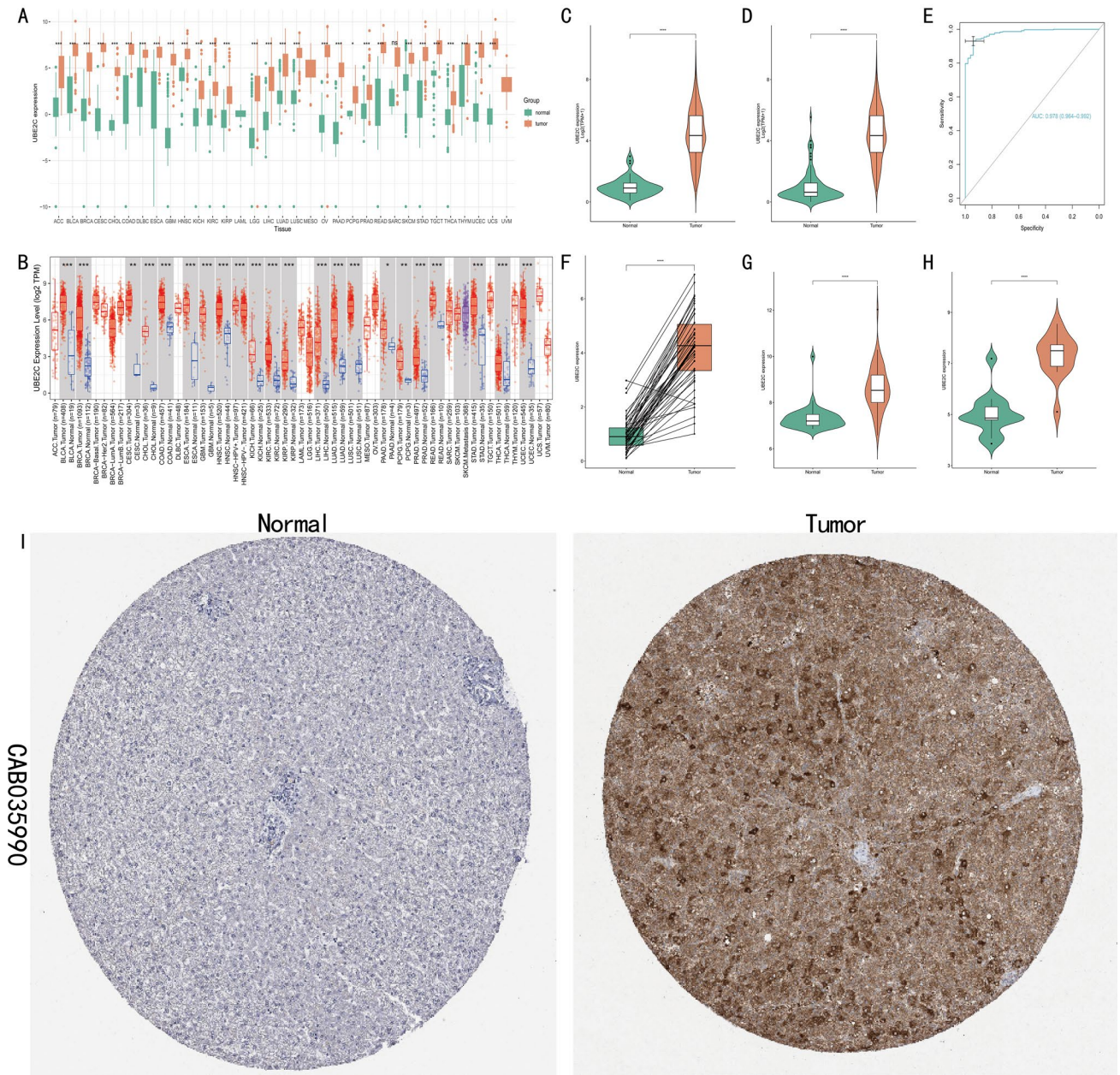

Fig. 2 Expression profile of UBE2C in malignant tumors. **A** Tumor samples (TCGA database) and normal samples (GTEx database). **B** TIMER2.0 database. UBE2C expression in LIHC samples and neighboring normal samples (**C**–**I**). **C** TCGA database. **D** Tumor samples (TCGA database) and normal samples (GTEx database). **E** Receiver operating characteristic curves for LIHC tissue and normal tissue samples. **F** Differential expression between LIHC samples and neighboring samples. **G** Validation of UBE2C expression in LIHC samples and neighboring normal samples (GSE121248). **H** Validation of UBE2C expression in LIHC samples and neighboring normal samples (GSE84402). **I** UBE2C protein was higher in LIHC tissues than normal tissues in the HPA database (antibody CAB011464). (*$p < 0.05$, **$p < 0.01$, ***$p < 0.001$, ****$p <$ 0.0001, and ns, no statistical difference)

Table 1 Comparison of *P*-values before and after Bonferroni treatment

ID	*P*-values	Bonferroni
TCGA	4.65E−28	1.86E−27
TACG-GTEx	4.35E−49	1.74E−48
GSE121248	2.22E−11	8.88E−11
GSE84402	0.00000693	2.77E−05

Fig. 3 Relationship between UBE2C expression and clinicopathologic features of HCC (**A**–**H**). **A** Histologic grade. **B** Gender. **C** Age. **D** OS event. **E** Pathologic stage. **F** T-stage. **G** N-stage. **H** M-stage. Prognostic analysis of UBE2C expression (**I**–**N**). **I** Disease-free interval. **J** Disease-specific survival. **K** Overall survival. **L** Progression-free interval. **M** Column line plot based on multivariate analysis with UBE2C expression and clinical characteristics. **N** Calibration plots showing model prediction accuracy.(*$p < 0.05$, **$p < 0.01$, ***$p < 0.001$, ****$p < 0.0001$, and ns, no statistical difference)

(1.81–4.40), $p < 0.001$), T stage (OR = 1.92 (1.18–3.11), $p = 0.008$), but correlated with sex (OR = 1.45 (0.94–2.24), $p = 0.097$), N stage (OR = 2.64 (0.27–25.74), $p = 0.403$) and M stage (OR = 0.28 (0.03–2.71), $p = 0.271$) correlations were not statistically significant (Table 3). These results indicate a correlation between the expression of UBE2C and the clinical characteristics of HCC.

3.3 Prognostic relevance of UBE2C expression

As shown by the Kaplan-Meier survival curves, the high UBE2C expression group was associated with a poor prognosis of HCC, with a high correlation between DFI (HR (95% CI) = 1.718 [1.192, 2.477], $p = 0.00129$, Fig. 3I), DSS (HR (95% CI) = 2.244 [1.374, 3.663], $p = 0.00022$, Fig. 3J), OS (HR (95% CI) = 1.870 [1.276, 2.741], $p = 0.00031$, Fig. 3K), and PFI (HR (95% CI) = 1.704 [1.227, 2.367], $p = 0.00040$, Fig. 3L). The association between UBE2C expression and poor prognosis in HCC was demonstrated by Cox univariate and multivariate analysis (Table 4). In addition, a clinical prognostic risk score model for HCC was constructed by using T-stage, N-stage, M-stage, age, gender, histologic grading, pathologic stage, and UBE2C expression (Fig. 3M). The accuracy of the prediction model was also assessed by calibration plots (Fig. 3N). UBE2C expression was a good predictor of 3- and 5-year survival probabilities. In summary, UBE2C expression was associated with poor prognoses in HCC patients.

3.4 Functional enrichment of UBE2C co-expressed genes

To investigate the potential function of UBE2C in HCC patients, patients with high and low UBE2C expression in the TCGA-LIHC dataset were analyzed using the "limma" package, and a total of 106 co-expressed genes were identified using $|\text{LogFC}| > 1.5$ and $p < 0.05$ as the screening criterion (Fig. 4A, Supplementary Table 1). The PPI network showed that CCNB1, CDK1, and FOXM1 were the top 3 proteins that significantly interacted with UBE2C (Fig. 4C). GO enrichment analysis revealed that UBE2C co-expressed genes were significantly enriched in biological processes (BP) such as cell cycle-related processes (such as chromosome segregation and mitosis), organelle fission, drug metabolism processes, and epoxygenase P450 pathway. In addition, it was significantly enriched in molecular functions such as iron ion binding and various enzyme activities (Fig. 4B). Analysis in KEGG enrichment showed that UBE2C co-expressed genes were enriched in signaling pathways such as cell cycle, retinol metabolism, chemical carcinogens, drug metabolism, steroid hormone biosynthesis, bile secretion, linoleic acid metabolism, and tyrosine metabolism (Fig. 4G). Furthermore, the ClueGo plugin in Cytoscape was utilized to evaluate the interrelationships among the enriched signaling pathways linked to UBE2C co-expressed genes (Fig. 4D). The results of the GSEA enrichment analysis showed that the top five pathways of the down-regulated genes associated with UBE2C were enriched in the complement and coagulation cascade, drug metabolism, metabolism of cytochromes to xenobiotics, metabolism, and steroid hormone biosynthesis (Fig. 4E); the top 5 pathways of UBE2C-related up-regulated genes were enriched for cell cycle-related processes (Fig. 4F). Finally, the correlations between UBE2C and these genes were analyzed. The results showed that UBE2C was associated with cell cycle-related genes (Fig. 5A–C), and UBE2C may interact with these genes to promote HCC development. And the correlation between UBE2C and cell cycle-related genes was verified by GSE121248 dataset (Fig. 6A–C).

3.5 Association of UBE2C high and low expression groups with somatic mutations

Somatic mutation data of the UBE2C gene were detected in 365 HCC patients in the TCGA database. The waterfall plot showed that the somatic mutation rate of patients in the high-expression group was 91.85% (169/184), with a high frequency of mutations in TP53 and TTN (Fig. 7A). The somatic mutation rate of patients in the low-expression group was 90.61% (164/181), with higher mutation frequencies of CTNNB1 and TTN (Fig. 7B). Different UBE2C expression groups showed significant pathway enrichment, and UBE2C exhibited somatic gene mutations in cancer-related signaling pathways such as RTK-RAS, TP53, WNT, Hippo, and NOTCH (Fig. 7C, D), which suggests that it plays a vital role in cancer development. Missense mutations occurred most in the UBE2C high and low expression groups, followed by Frame_Shift_Del.

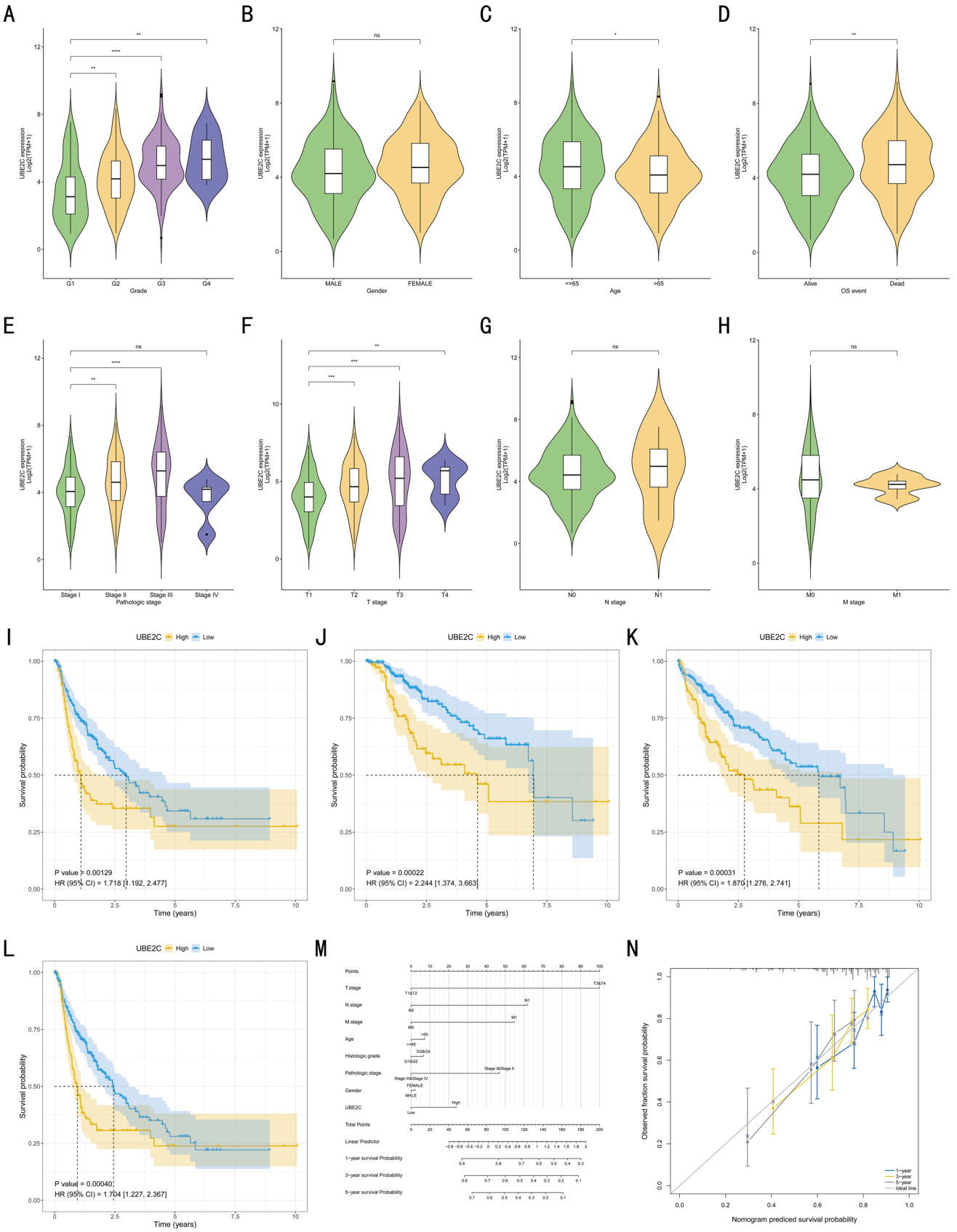
A
B
C
D
E
F
G
H
UBE2C expression Log2(TPM+1)
Grade
G1
G2
G3
G4
Gender
MALE
FEMALE
Age
<=65
>65
OS event
Alive
Dead
Pathologic stage
Stage I
Stage II
Stage III
Stage IV
T stage
T1
T2
T3
T4
N stage
N0
N1
M stage
M0
M1
I
J
K
L
UBE2C High Low
Survival probability
Time (years)
P value = 0.00129
HR (95% CI) = 1.718 [1.192, 2.477]
P value = 0.00022
HR (95% CI) = 2.244 [1.374, 3.663]
P value = 0.00031
HR (95% CI) = 1.870 [1.276, 2.741]
P value = 0.00040
HR (95% CI) = 1.704 [1.227, 2.367]
M
Points
T.stage
N.stage
M.stage
Age
Histologic.grade
Pathologic.stage
Gender
UBE2C
Total Points
Linear Predictor
1-year survival Probability
3-year survival Probability
5-year survival Probability
N
Observed fraction survival probability
Nomogram prediced survival probability
1-year
3-year
5-year
Ideal line

Table 2 Relationship between UBE2C expression and clinicopathologic features of HCC patients

Characteristic	Low expression of UBE2C	High expression of UBE2C	*p*
n	185	185	
Age, n(%)			0.024
<= 65	105 (56.8%)	127 (68.6%)	
> 65	80 (43.2%)	58 (31.4%)	
Gender, n(%)			0.121
Female	53 (28.6%)	68 (36.8%)	
Male	132 (71.4%)	117 (63.2%)	
T stage, n(%)			0.001
T1	109 (59.9%)	72 (38.9%)	
T2	38 (20.9%)	55 (29.7%)	
T3	30 (16.5%)	50 (27.0%)	
T4	5 (2.75%)	8 (4.32%)	
N stage, n(%)			0.626
N0	118 (99.2%)	134 (97.8%)	
N1	1 (0.84%)	3 (2.19%)	
M stage, n(%)			0.336
M0	121 (97.6%)	145 (99.3%)	
M1	3 (2.42%)	1 (0.68%)	
Pathologic stage, n(%)		< 0.001	
Stage I	102 (59.3%)	69 (39.7%)	
Stage II	37 (21.5%)	48 (27.6%)	
Stage III	29 (16.9%)	56 (32.2%)	
Stage IV	4 (2.33%)	1 (0.57%)	
Histologic grade, n(%)		< 0.001	
G1	42 (23.1%)	13 (7.10%)	
G2	95 (52.2%)	82 (44.8%)	
G3	41 (22.5%)	80 (43.7%)	
G4	4 (2.20%)	8 (4.37%)	

Table 3 Logistic regression analysis of UBE2C expression

Characteristics	Total(N)	Odds ratio(OR)	*p*-value
Age (<= 65 vs. > 65)	370	1.67 (1.09–2.55)	0.018
Gender (Male vs. Female)	370	1.45 (0.94–2.24)	0.097
Pathologic stage (stage I and stage II vs. stage III and stage IV)	346	2.05 (1.25–3.36)	0.004
Histologic grade (G1 and G2 vs. G3 and G4)	365	2.82 (1.81–4.40)	<0.001
T stage	367	1.92 (1.18–3.11)	0.008
N stage	256	2.64 (0.27–25.74)	0.403
M stage	270	0.28 (0.03–2.71)	0.271

SNP mutations were the most common type, with C>T and C>A accounting for 48.5% and 47.2% of SNP mutations in the UBE2C high and low expression groups, respectively (Fig. 7E, F).

3.6 Relationship between UBE2C high and low expression groups and the seven steps of the anti-tumor immune cycle

The genes characterizing the seven steps of the anti-tumor immune cycle were downloaded and analyzed through the TIP database (Supplementary Table 2). Compared with the UBE2C low-expression group, the release of cancer cell antigens (step 1) was significantly higher in the UBE2C high-expression group. However, there were no significant difference

Table 4 Univariate and multivariate Cox regression analysis of clinical characteristics

Characteristic		Univariable		Multivariable	
		HR (95% CI)	*p*	HR (95% CI)	*p*
OS	Age	1.01 (1.00–1.03)	0.078		
	Gender (Male vs. Female)	1.23 (0.86–1.75)	0.26		**<0.001**
	Pathologic stage (stage I and stage II vs. stage III and stage IV)	2.45 (1.69–3.55)	<0.001	1.45 (0.20–10.66)	0.716
	Histologic grade (G1 and G2 vs. G3 and G4)	1.12 (0.78–1.61)	0.539		
	T stage (T1 and T2 vs. T3 and T4)	2.54 (1.78–3.61)	<0.001	1.78 (0.24–13.08)	0.572
	N stage (N0 vs. N1)	2.00 (0.49–8.16)	0.334		
	M stage (M0 vs. M1)	4.03 (1.27–12.83)	0.018	2.75 (0.80–9.38)	0.107
	UBE2C (Low vs. High)	1.44 (1.01–2.03)	0.041	1.60 (1.01–2.56)	0.072
DSS	Age	1.00 (0.99–1.02)	0.724		
	Gender (MALE vs. FEMALE)	1.19 (0.76–1.88)	0.452		
	Pathologic stage (stage I and stage II vs. stage III and Stage IV)	3.71 (2.28–6.01)	<0.001	2.44 (0.32–18.46)	0.389
	Histologic grade (G1 and G2 vs. G3 and G4)	1.12 (0.70–1.78)	0.635		
	T stage (T1 and T2 vs. T3 and T4)	3.54 (2.27–5.54)	<0.001	1.49 (0.20–11.21)	0.696
	N stage (N0 vs. N1)	3.55 (0.85–14.72)	0.081		
	M stage (M0 vs. M1)	5.10 (1.23–21.16)	0.025	3.16 (0.69–14.50)	0.138
	UBE2C (Low vs. High)	1.67 (1.07–2.62)	0.025	1.82 (0.98–3.39)	0.059
DFI	Age	1.00 (0.98–1.01)	0.621		
	Gender (Male vs. Female)	0.85 (0.60–1.22)	0.385		
	Pathologic stage (stage I and stage II vs. stage III and stage IV)	2.36 (1.63–3.41)	<0.001	0.98 (0.14–7.08)	0.983
	Histologic grade (G1 and G2 vs. G3 and G4)	1.23 (0.88–1.73)	0.222		
	T stage (T1 and T2 vs. T3 and T4)	2.36 (1.65–3.38)	<0.001	2.39 (0.33–17.46)	0.391
	N stage (N0 vs. N1)	1.58 (0.39–6.41)	0.524		
	UBE2C (Low vs. High)	1.56 (1.12–2.17)	0.009	1.45 (1.03–2.05)	**0.035**
PFI	Age	1.00 (0.98–1.01)	0.421		
	Gender (MALE vs. FEMALE)	1.03 (0.75–1.40)	0.861		
	Pathologic stage (stage I and stage II vs. stage III and stage IV)	2.21 (1.60–3.07)	<0.001	1.48 (0.36–6.17)	0.588
	Histologic grade (G1 and G2 vs. G3 and G4)	1.15 (0.85–1.56)	0.356		
	T stage (T1 and T2 vs. T3 and T4)	2.19 (1.59–3.00)	<0.001	1.40 (0.34–5.85)	0.645
	N stage (N0 vs. N1)	1.39 (0.34–5.61)	0.648		
	M stage (M0 vs. M1)	3.44 (1.08–10.97)	0.037	2.70 (0.81–8.98)	0.106
	UBE2C (Low vs. High)	1.55 (1.16–2.09)	0.003	1.52 (1.05–2.18)	**0.025**

in cancer antigen presentation and priming and activation (steps 2 and 3) (Fig. 8A). For step 4, the chemotaxis ability of TH22 cells, and Treg cells in the high-expression group was significantly more potent than that of the low-expression group (Fig. 8B). Next, infiltration of immune cells into tumors, recognition of cancer cells by T cells and killing of cancer cells were significantly lower in the high-expression group than in the low-expression group (steps 5–7) (Fig. 8C). This result may indicate that HCC may survive and proliferate by using immune checkpoints to evade surveillance by the immune system.

3.7 Relationship between UBE2C expression and immune cell infiltration

The immune infiltration of the tumors was analyzed based on 16 different types of immune cells and 13 marker genes for immune function scores obtained from the study of He et al. and using the "GSVA" and "CIBERSORT" software packages, respectively. The results of immune infiltration showed that UBE2C expression was significantly different from a variety of immune cell infiltrations. Among them, those that showed positive correlation were aDCs (R = 0.29, p = 1.8e−08), Dendritic cells resting (R = 0.18, p = 0.00047), iDCs (R = 0.12, p = 0.021), Macrophages M0 (R = 0.24, p = 2.9e−06), Tfh (R = 0.23, p = 1e−05), Tregs (R = 0.25, p = 1e−06), and also presenting negative correlations were Macrophages M2 (R =− 0.25, p = 9e−07), Mast cells (R =− 0.2, p = 6.8e−05), Monocytes (R =− 0.2, p = 0.00014), NK cells (R =− 0.23, p = 8.9e−06)

Fig. 4 Differential expression and functional enrichment analysis of UBE2C genes (**A**–**C**). **A** Volcano plot of UBE2C expression patterns illustrating differentially co-expressed genes. **B** Top 8 terms of UBE2C co-expressed genes based on the GO analysis, including biological process (BP), cellular component (CC), and molecular function (MF) terms. **C** PPI network of UBE2C differentially co-expressed genes. GSEA enrichment analysis of UBE2C differentially co-expressed genes (**D**–**G**). **D** UBE2C co-expressed gene enrichment signaling pathways and interactions between pathways. **E**, **F** UBE2C up-regulates or down-regulates the top five pathways of related genes. **G** KEGG-enriched pathway of UBE2C-related genes

(Figs. 9A–C, 10). In addition, immunofunctional analyses showed that UBE2C expression was significantly different from APC co-stimulation, Type I IFN Response and Type II IFN Response (Fig. 9D) and significantly different from Type I IFN Response (R =– 0.22, p = 1.9e–05), Type II IFN Response (R =– 0.52, p < 2.2e–16) showed negative correlation (Fig. 9F).

3.8 Relationship between UBE2C and tumor immune microenvironment

The relationship between the differential expression of UBE2C and inhibitory immune molecules was investigated based on the TISIDB database. The findings revealed that IL10RB, LAG3, CTLA4, HAVCR2, TGFB1, TGFBR1, LGALS9, PDCD1, TIGIT, and VTCN1 exhibited significant up-regulation in the UBE2C high-expression group, while KDR demonstrated significant down-regulation (p < 0.001) (Fig. 9E), and validated the relationship between UBE2C and immunosuppressive molecules in the GSE121248 dataset (Fig. 6D). Then, the results of the correlation between UBE2C and immunotherapy efficacy showed that the TIDE score and T-cell exclusion rate were higher in the UBE2C high-expression group (Fig. 9G, H). In contrast, the T-cell dysfunction score was reduced (Fig. 9I), and it was significantly different from MDSC, CD8 and MSI (p < 0.001) (Fig. 11). In addition, patients with high UBE2C expression had relatively lower stromal scores and estimated scores and relatively higher immune scores and patient tumor purity. However, UBE2C expression was only significantly different from the stromal score (Fig. 9J–M).

To investigate the involvement of UBE2C in the HCC immune microenvironment, the relationship between UBE2C expression and immune microenvironment parameters was assessed using the TISIDB database (Fig. 12, Supplementary Table 3). According to Fig. 12, the immunostimulants with the strongest correlation with UBE2C: CD276 (R = 0.54, p < 0.001), TNFRSF18 (R = 0.42, p < 0.001) (Fig. 12A); Chemokines: XCL1 (R = 0.36, p < 0.001), CCL20 (R = 0.35, p < 0.001) (Fig. 12B); MHC molecules: TAP1 (R = 0.27, p <0.001), TAPBP (R = 0.22, p < 0.001) (Fig. 12C); Immunosuppressants: PDCD1 (R = 0.36, p < 0.001), CTLA4 (R = 0.35, p < 0.001) (Fig. 12D); Chemokine receptors: CCR10 (R = 0.51, p < 0.001), CXCR3 (R = 0.29, p < 0.001) (Fig. 12E). All these results suggest that UBE2C is likely to play a complex regulatory role in the immune microenvironment of HCC.

4 Discussion

Cancer presently ranks as the primary or secondary cause of untimely mortality in the majority of nations across the globe. By 2070, the prevalence of all types of cancer is projected to increase twofold in comparison to the year 2020 [30]. Previous studies have found that tumor development and progression are closely related to metabolic abnormalities and alterations in the immune microenvironment. There is evidence that metabolism plays a significant role in tumorigenesis and development [31]. For example, lipid and glutamine metabolism have been implicated in tumorigenesis and development [32].

Recent studies have shown that UBE2C gene expression is significantly up-regulated in a variety of tumors compared to normal tissue samples [33], and UBE2C gene expression levels are associated with many types of tumors, with UBE2C being almost undetectable in normal tissues [34, 35]. Although several studies have demonstrated the differential expression and function of UBE2C genes in tumors [36, 37], there are fewer studies on UBE2C gene expression associated with immunotherapy response. Therefore, this study performed ROC and Wilcoxon analyses on the training and validation datasets. These analyses aimed to confirm the expression level of UBE2C in HCC and its diagnostic utility. The results showed higher levels of UBE2C expression were exhibited in HCC compared to controls. Notably, the AUC values in the RPC analysis exceeded 0.9, highlighting the great potential of UBE2C as a biomarker for diagnosing and treating HCC. In addition, according to Figs. 2F and 7 results, UBE2C was differentially expressed in tumor tissues and adjacent normal tissues, and different UBE2C expressions exhibited different somatic mutation expression profiles. For example, TP53 mutation was highest in the high expression group, while CTNNB1 mutation was highest in the low expression group. It has been shown that UBE2C can be used as a prognostic biomarker for some tumors, such as prostate cancer [38] and breast cancer [39]. Prior research has demonstrated

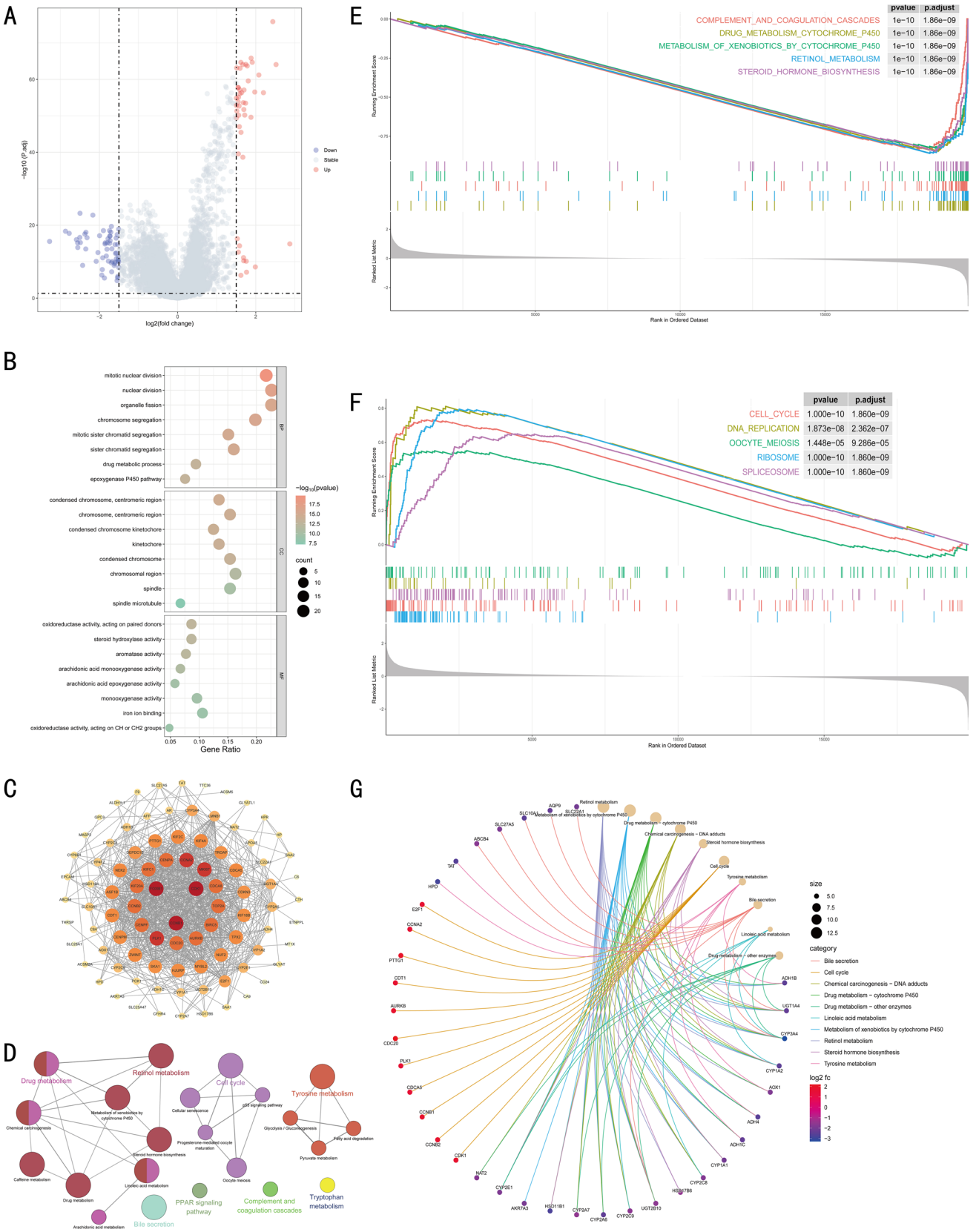
A
−log10 (P.adj)
log2(fold change)
Down
Stable
Up
B
mitotic nuclear division
nuclear division
organelle fission
chromosome segregation
mitotic sister chromatid segregation
sister chromatid segregation
drug metabolic process
epoxygenase P450 pathway
condensed chromosome, centromeric region
chromosome, centromeric region
condensed chromosome kinetochore
kinetochore
condensed chromosome
chromosomal region
spindle
spindle microtubule
oxidoreductase activity, acting on paired donors
steroid hydroxylase activity
aromatase activity
arachidonic acid monooxygenase activity
arachidonic acid epoxygenase activity
monooxygenase activity
iron ion binding
oxidoreductase activity, acting on CH or CH2 groups
BP
CC
MF
−log10(pvalue)
count
Gene Ratio
C
D
Drug metabolism
Retinol metabolism
Cell cycle
Tyrosine metabolism
Chemical carcinogenesis
Metabolism of xenobiotics by cytochrome P450
Cellular senescence
p53 signaling pathway
Glycolysis / Gluconeogenesis
Fatty acid degradation
Steroid hormone biosynthesis
Progesterone-mediated oocyte maturation
Pyruvate metabolism
Caffeine metabolism
Linoleic acid metabolism
Oocyte meiosis
Drug metabolism
Arachidonic acid metabolism
PPAR signaling pathway
Complement and coagulation cascades
Tryptophan metabolism
Bile secretion
E
pvalue
p.adjust
COMPLEMENT_AND_COAGULATION_CASCADES 1e−10 1.86e−09
DRUG_METABOLISM_CYTOCHROME_P450 1e−10 1.86e−09
METABOLISM_OF_XENOBIOTICS_BY_CYTOCHROME_P450 1e−10 1.86e−09
RETINOL_METABOLISM 1e−10 1.86e−09
STEROID_HORMONE_BIOSYNTHESIS 1e−10 1.86e−09
Running Enrichment Score
Ranked List Metric
Rank in Ordered Dataset
F
pvalue
p.adjust
CELL_CYCLE 1.000e−10 1.860e−09
DNA_REPLICATION 1.873e−08 2.362e−07
OOCYTE_MEIOSIS 1.448e−05 9.286e−05
RIBOSOME 1.000e−10 1.860e−09
SPLICEOSOME 1.000e−10 1.860e−09
Running Enrichment Score
Ranked List Metric
Rank in Ordered Dataset
G
Retinol metabolism
Metabolism of xenobiotics by cytochrome P450
Drug metabolism − cytochrome P450
Chemical carcinogenesis − DNA adducts
Steroid hormone biosynthesis
Cell cycle
Tyrosine metabolism
Bile secretion
Linoleic acid metabolism
Drug metabolism − other enzymes
size
category
Bile secretion
Cell cycle
Chemical carcinogenesis − DNA adducts
Drug metabolism − cytochrome P450
Drug metabolism − other enzymes
Linoleic acid metabolism
Metabolism of xenobiotics by cytochrome P450
Retinol metabolism
Steroid hormone biosynthesis
Tyrosine metabolism
log2 fc

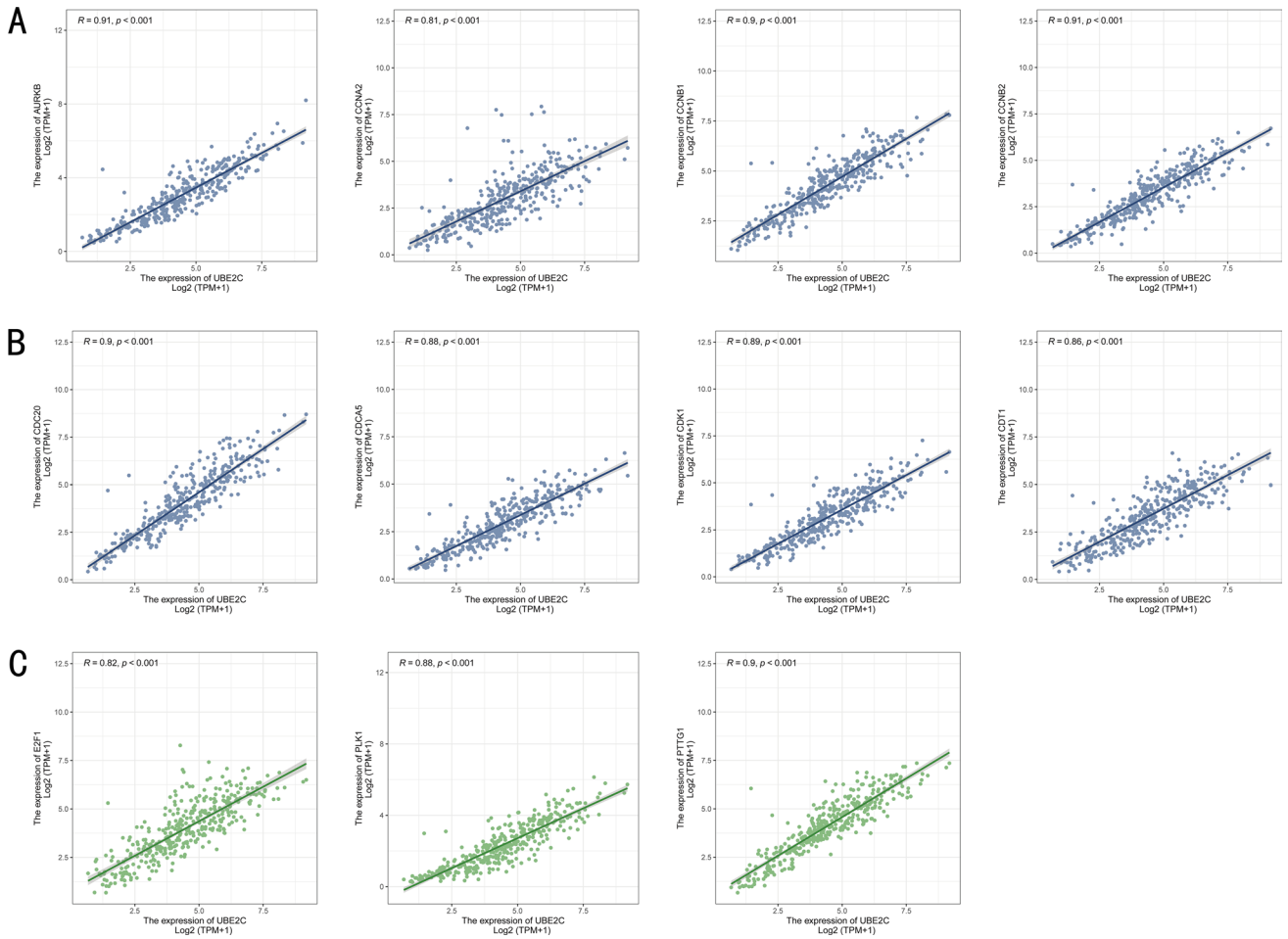

Fig. 5 Relationship between UBE2C and cell cycle-related genes. **A**–**C** Correlation of UBE2C with gene expression in the TCGA database

that the overexpression of UBE2C leads to chromosome mismatches and alters the cell cycle mechanism, thereby facilitating cellular proliferation [40, 41]. This suggests high UBE2C expression may promote HCC cell proliferation by altering cell cycle mechanisms.

In this study, we systematically described the associations between UBE2C and the clinical characteristics of HCC patients, prognostic associations with four survival endpoints, and associations with the immune microenvironment and its factors. By immunohistochemistry, UBE2C protein expression was significantly increased in tumor tissues compared to normal tissue samples. In addition, high expression of UBE2C was found to be significantly associated with OS, DSS, DFI, and PFI in HCC patients. Taken together, UBE2C may serve as a prognostic marker for HCC. In studies related to clinical features, UBE2C was significantly correlated with pathological stage, histologic grading, and T-stage. UBE2C expression was significantly correlated with DFI and PFI, as shown by unifactorial and multifactorial Cox survival analysis, suggesting that UBE2C may be a reliable marker of prognosis in HCC patients.

In the G2/M phase of the cell cycle, CCNB1 and CCNB2 can map CDK1 to form a complex that regulates mitotic initiation [42]. It has also been shown that high CCNB1, CCNB2 and CDK1 expression is associated with a poor prognosis in HCC patients [43]. Existing studies have shown that CCNB1 and CCNB2 play an essential role in mediating the G2/M transition in the cell cycle [44]. In addition, it has been shown that CCNA2 expression is similarly reduced after silencing UBE2C [45], which is consistent with our results. The G2/M transition in eukaryotes is mainly regulated by the CDK1/Cyclin B1 complex, and depletion of CDK1 leads to blockade of the G2/M transition [46, 47]. Interestingly, UBE2C expression levels were significantly and positively correlated with CCNB1, CCNB2, CDK1, and CCNA2 expression levels. Similarly, GO and KEGG enrichment analyses showed that UBE2C may regulate HCC development through cell cycle-related pathways and biological processes. This suggests that UBE2C may mediate the G2/M transition in the cell cycle by promoting CCNB1, CCNB2 and CDK1, which in turn promotes the proliferation and development of HCC.

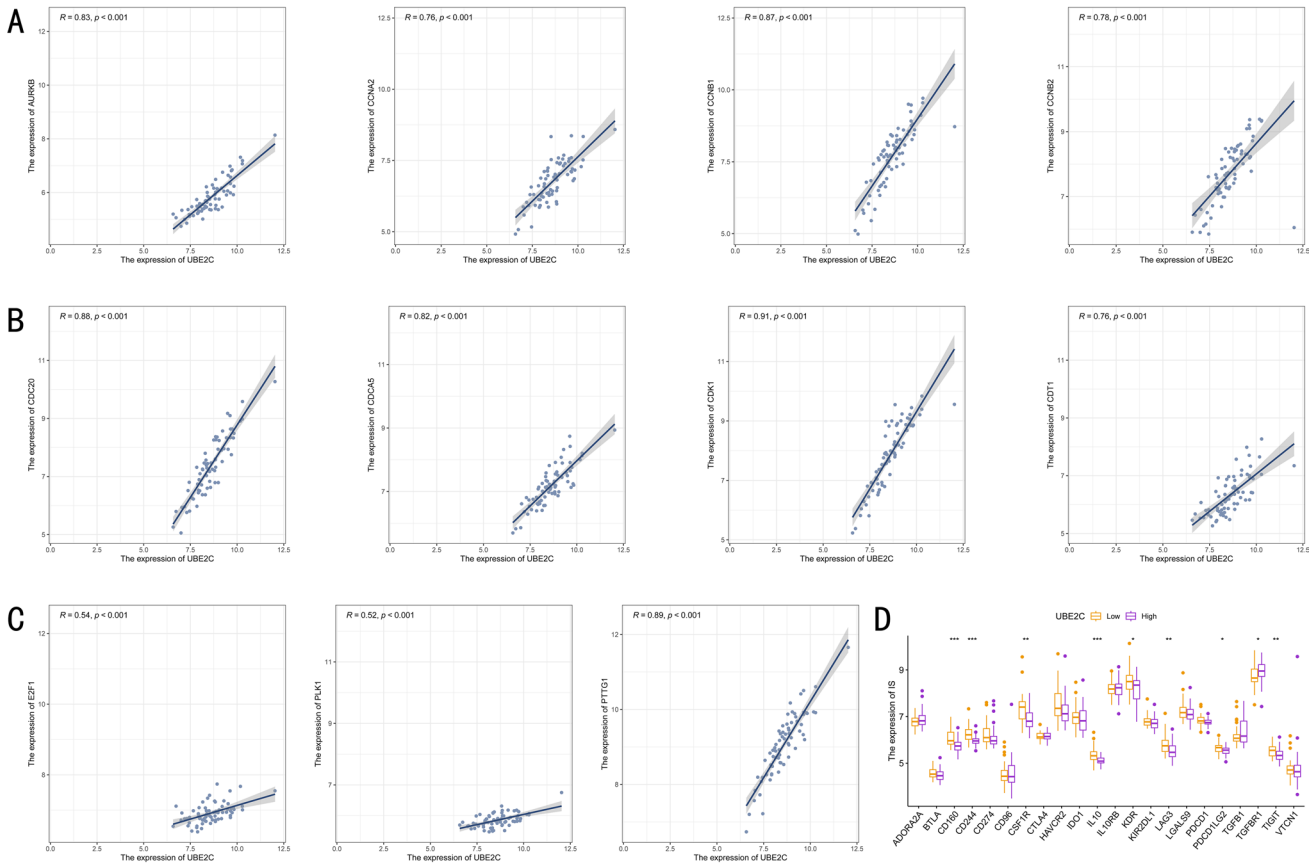

Fig. 6 Relationship of UBE2C to cell cycle-related genes and immunosuppressive molecules. **A**–**C** Correlation of UBE2C with cell cycle-related gene expression in the GSE121248 dataset. **D** Relationship between UBE2C and immunosuppressive molecules in the GSE121248 dataset

In this study, we innovatively and systematically introduced the correlation between UBE2C expression and the tumor immune microenvironment in HCC patients. The investigation revealed that many dendritic cells, regulatory T cells, and macrophages invaded the UBE2C high-expression group. These cells were found to control the immune milieu and facilitate tumor growth in specific circumstances. It has been shown that Treg cells maintain immune tolerance in tumor tissues through immunosuppressive effects, thus exerting immunosuppressive effects and allowing tumor cells to evade immune killing [48, 49]. Thus, UBE2C can influence the infiltration of immune cells by directly or indirectly regulating the tumor immune microenvironment. Most importantly, high UBE2C expression correlates highly with the immune checkpoints PDCD1 (PD-1) and CTLA4. PD-1 binds to PD-L1 on tumors and can street effective inhibitory signals, an effect that has a detrimental impact on anti-tumor immunity [50]. CTLA4 is expressed primarily on activated T cells and can restrict APCs through competitive binding of interactions between surface-expressed CD28 and CD80/CD86, leading to immunosuppression [51]. Based on these findings, it is hypothesized that high expression of UBE2C may competitively inhibit the antigen presentation function of APC by promoting the cell surface factor CTLA4. At the same time, it may also promote HCC immune evasion by facilitating the binding of PD-1 to PD-L1 and thus HCC immunity. Interestingly, high expression of UBE2C implies a high immunity score in KIRC and a decreased level of CD4 T cell and macrophage infiltration in LUAD [52, 53]. However, the results of the present study showed that UBE2C expression was not statistically different from the immunity score and showed a positive correlation with CD4 T cells and macrophages. This demonstrated the differential role of UBE2C in different tumor tissues.

The immunosuppressive environment of HCC is known to have pro-tumorigenic properties [54]. MDSC, as a representative immunosuppressive component in HCC, promotes tumor cell survival and proliferation, accelerates tumor vascular growth and metastasis, and suppresses anti-tumor immune responses [55]. MDSC can suppress T-cell activity by expressing a series of effector molecules containing chemokines (e.g., CCL3, CCL4, CCL5) effector molecules to inhibit T cell activity [56]. According to Figs. 11 and 12, UBE2C showed a positive correlation with these chemokines, and MDSC

Fig. 7 Genetic variation of UBE2C in LIHC from the TCGA database. **A**, **B** Mutation frequencies of UBE2C high (**A**) and low (**B**) expression groups in 365 HCC patients according to the TCGA dataset. Each column represents one patient, the bar at the top represents TMB, and the numbers on the right represent the mutation frequencies of the top 30 common genes in the corresponding groups. **C** Enriched pathways for UBE2C mutations in the high expression group. **D** Enrichment pathways of UBE2C mutations in the low expression group. **E**, **F** Mutation distribution maps of different expression groups, including mutation classification statistics, mutation type statistics, single nucleotide polymorphism mutation breakdown statistics, mutation number and proportion statistics of all samples, number statistics of different mutation types, and statistics of most mutated genes in the high (**E**) and low (**F**) expression groups. Where A: adenine, C: cytosine, G: guanine, T: thymine

levels were elevated in the high-expression group. Based on these findings, it is hypothesized that high expression of UBE2C may promote T cell activity inhibition by elevating MDSC levels and promoting chemokine release, promoting HCC survival. However, the more precise mechanism of UBE2C on the immune microenvironment of HCC remains to be elucidated. Cancer immunotherapy, especially immune checkpoint blockade therapy, is a standard treatment for various malignancies by promoting complete and sustained immune responses to alter cancer treatment. Unfortunately, only a small percentage of patients respond to immunotherapy, possibly due to insufficient immune activation to recognize tumor-specific antigens [57]. Therefore, it is crucial to identify other potential therapeutic targets. The current study shows that UBE2C levels strongly correlate with multiple immune checkpoints in HCC, suggesting that UBE2C may be an immune-related therapeutic target for HCC patients. The present study points to a new direction for the relationship between the ubiquitin-binding enzyme-related gene UBE2C and immune cell infiltration within the TME, which is of great significance in exploring new strategies for immunotherapy of HCC.

However, this study has some limitations. First, all data in this study were obtained from online databases; further studies on the samples are needed to confirm our results. Reliance on publicly available databases raises the possibility of systematic bias. Because public datasets may inherently carry some variance, any systematic bias present in these data could potentially affect the results of our analysis. It is crucial to recognize this limitation as he may introduce uncertainty to the generalizability and reliability of our conclusions. Second, while most of the algorithms employed in this study are stable and rigorous, it is essential to be aware of the inherent limitations imposed by the current state of biology, that the stability of our conclusions may change at any time, and that future advances in bioinformatics may introduce new insights or alter existing interpretations, which underscores the need for ongoing review and validation of our findings. In addition, most of the data in this study relied on the TCGA database and lacked other independent datasets for validation. The results may be more convincing if compared with other databases.

5 Conclusion

In this study, after bioinformatics analysis, it was shown that UBE2C was differentially expressed in HCC and normal tissues and was involved in the infiltration of immune cells in the tumor microenvironment. UBE2C can potentially be used as a biomarker and immunotherapeutic target for HCC. However, this study is mainly based on data analysis with some limitations, and further experiments are needed to validate and explore the potential mechanisms.

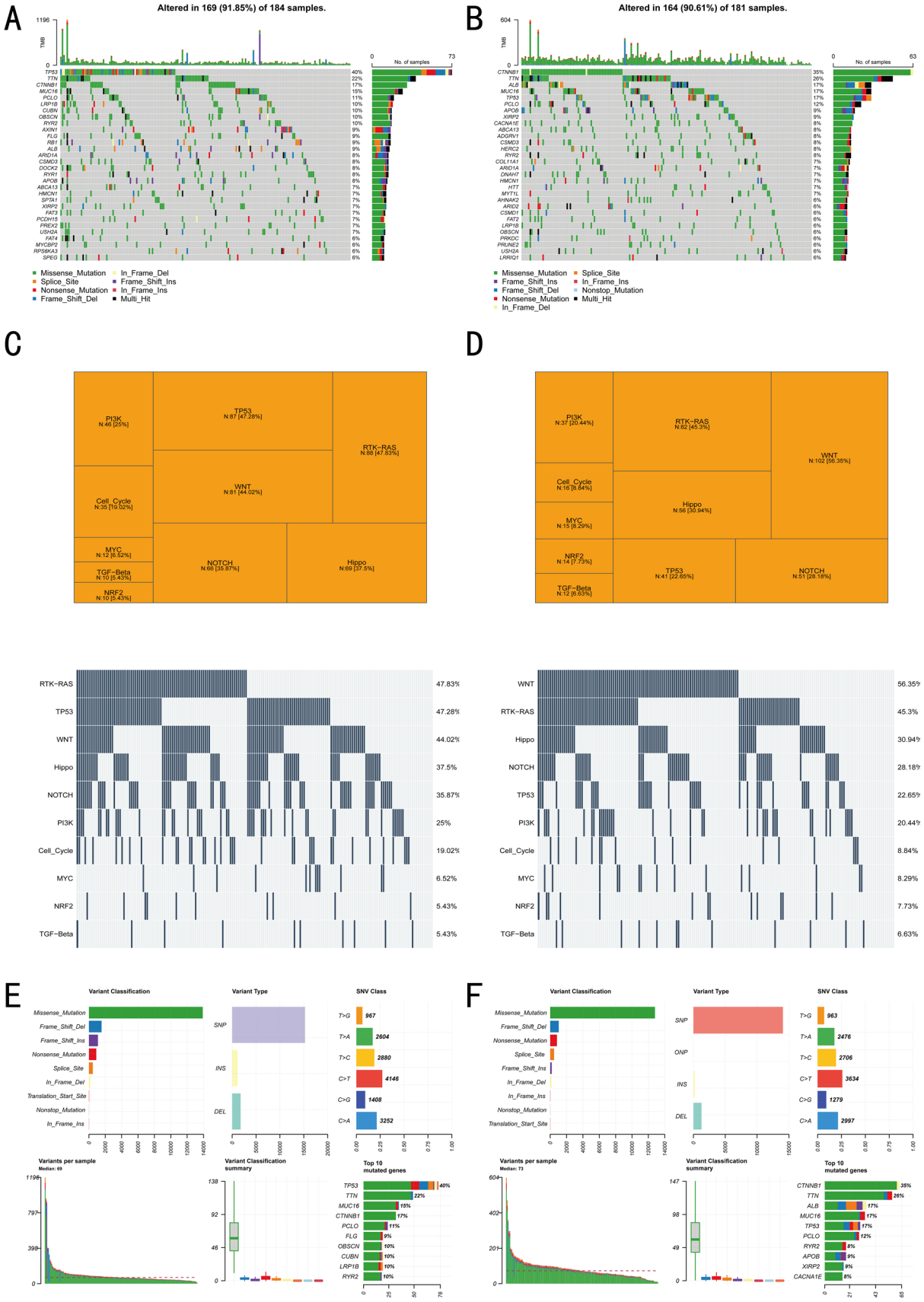
A
Altered in 169 (91.85%) of 184 samples.
TMB
No. of samples
Missense_Mutation
Splice_Site
Nonsense_Mutation
Frame_Shift_Del
In_Frame_Del
Frame_Shift_Ins
In_Frame_Ins
Multi_Hit
B
Altered in 164 (90.61%) of 181 samples.
TMB
No. of samples
Missense_Mutation
Frame_Shift_Ins
Frame_Shift_Del
Nonsense_Mutation
In_Frame_Del
Splice_Site
In_Frame_Ins
Nonstop_Mutation
Multi_Hit
C
PI3K N:46 [25%]
TP53 N:87 [47.28%]
RTK−RAS N:88 [47.83%]
Cell_Cycle N:35 [19.02%]
WNT N:81 [44.02%]
MYC N:12 [6.52%]
TGF−Beta N:10 [5.43%]
NRF2 N:10 [5.43%]
NOTCH N:66 [35.87%]
Hippo N:69 [37.5%]
RTK−RAS 47.83%
TP53 47.28%
WNT 44.02%
Hippo 37.5%
NOTCH 35.87%
PI3K 25%
Cell_Cycle 19.02%
MYC 6.52%
NRF2 5.43%
TGF−Beta 5.43%
D
PI3K N:37 [20.44%]
RTK−RAS N:82 [45.3%]
WNT N:102 [56.35%]
Cell_Cycle N:16 [8.84%]
Hippo N:56 [30.94%]
MYC N:15 [8.29%]
NRF2 N:14 [7.73%]
TP53 N:41 [22.65%]
NOTCH N:51 [28.18%]
TGF−Beta N:12 [6.63%]
WNT 56.35%
RTK−RAS 45.3%
Hippo 30.94%
NOTCH 28.18%
TP53 22.65%
PI3K 20.44%
Cell_Cycle 8.84%
MYC 8.29%
NRF2 7.73%
TGF−Beta 6.63%
E
Variant Classification
Missense_Mutation
Frame_Shift_Del
Frame_Shift_Ins
Nonsense_Mutation
Splice_Site
In_Frame_Del
Translation_Start_Site
Nonstop_Mutation
In_Frame_Ins
Variant Type
SNP
INS
DEL
SNV Class
T>G 967
T>A 2604
T>C 2880
C>T 4146
C>G 1408
C>A 3252
Variants per sample
Median: 69
Variant Classification summary
Top 10 mutated genes
TP53 40%
TTN 22%
MUC16 15%
CTNNB1 17%
PCLO 11%
FLG 9%
OBSCN 10%
CUBN 10%
LRP1B 10%
RYR2 10%
F
Variant Classification
Missense_Mutation
Frame_Shift_Del
Nonsense_Mutation
Splice_Site
Frame_Shift_Ins
In_Frame_Del
In_Frame_Ins
Nonstop_Mutation
Translation_Start_Site
Variant Type
SNP
ONP
INS
DEL
SNV Class
T>G 963
T>A 2476
T>C 2706
C>T 3634
C>G 1279
C>A 2997
Variants per sample
Median: 73
Variant Classification summary
Top 10 mutated genes
CTNNB1 35%
TTN 26%
ALB 17%
MUC16 17%
TP53 17%
PCLO 12%
RYR2 8%
APOB 9%
XIRP2 9%
CACNA1E 8%

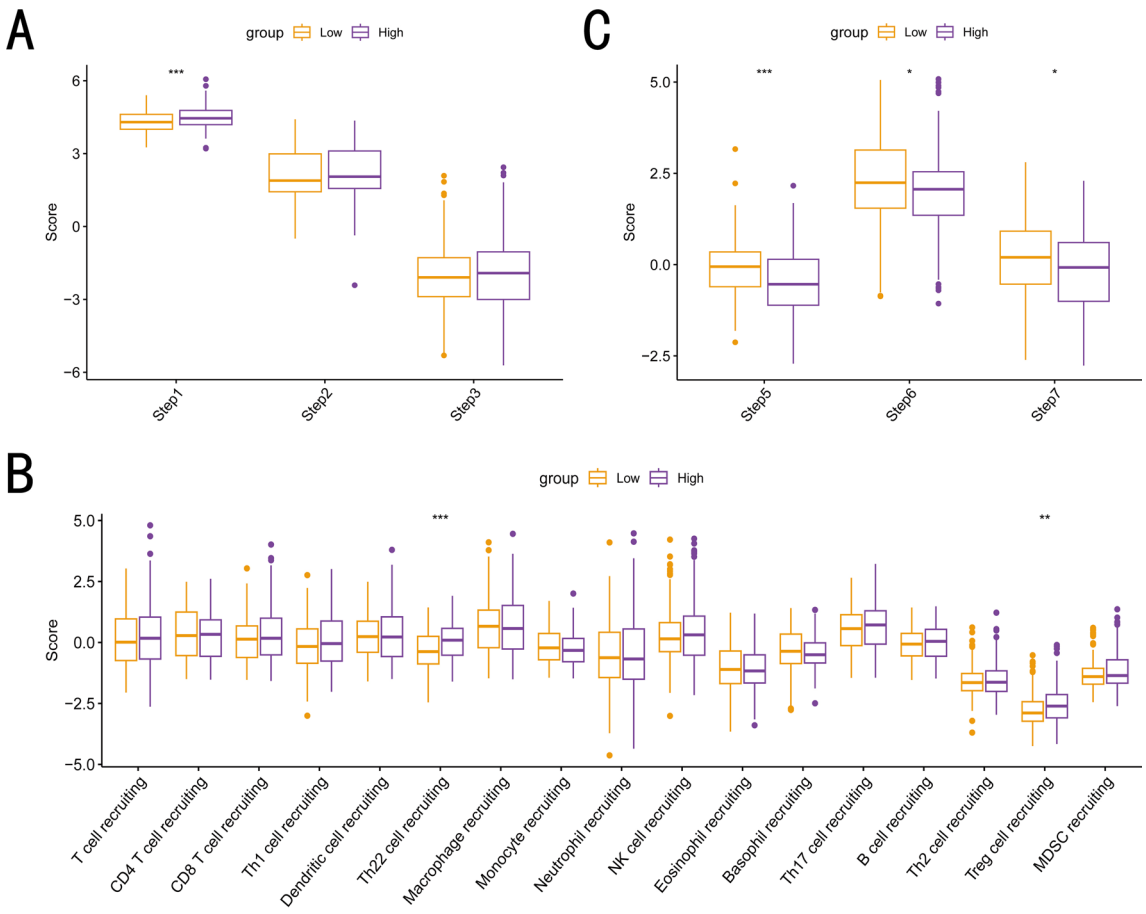

Fig. 8 Correlation of different expression groups of UBE2C with the seven steps of the cancer immune cycle. **A** Relationship between different expression groups of UBE2C and release of tumor antigen (step 1), presentation of tumor antigen (step 2) and initiation and activation of immune cells (step 3). **B** Relationship between different expression groups of UBE2C and the migration ability of T cells to tumor cells (step 4). **C** Relationship between UBE2C different expression groups and tumor tissue T cell infiltration (step 5), T cell recognition of tumor cells (step 6), and ability to clear tumor cells (step 7). (*$p < 0.05$, **$p < 0.01$, ***$p < 0.001$, and ns, no statistical difference)

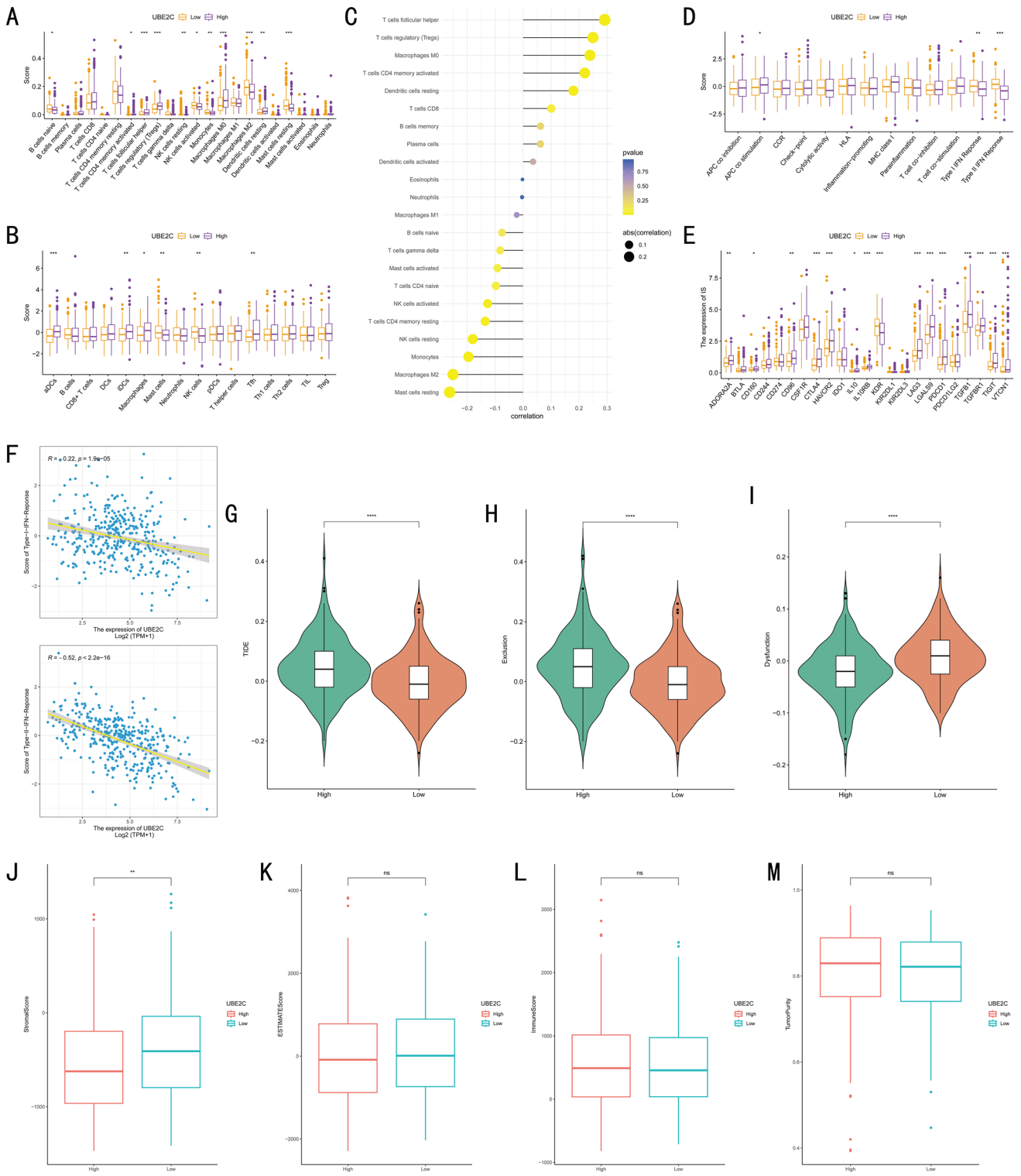

Fig. 9 Relationship between UBE2C and tumor immune microenvironment. **A** UBE2C high and low expression groups and immune cell infiltration (CIBERSORT). **B** Relationship between UBE2C high and low expression group and immune cell infiltration (ssGSEA). **C** Relationship between UBE2C expression and immune cell infiltration status. **D** Relationship between UBE2C high and low expression groups and immune function. **E** Relationship between UBE2C and immunosuppressive molecules. **F** Correlation between UBE2C expression and immune function. Immunotherapy response biomarkers (**G**–**I**), including tumor immune dysfunction and exclusion (TIDE) score (G), T-cell exclusion score (**H**) and T-cell dysfunction score (**I**), between UBE2C low and high expression group. High and low UBE2C expression groups with stromal score (**J**), estimated score (**K**), immune score (**L**) and tumor purity (**M**). (*$p < 0.05$, **$p < 0.01$, ***$p < 0.001$, ****$p < 0.0001$, and ns, no statistical difference)

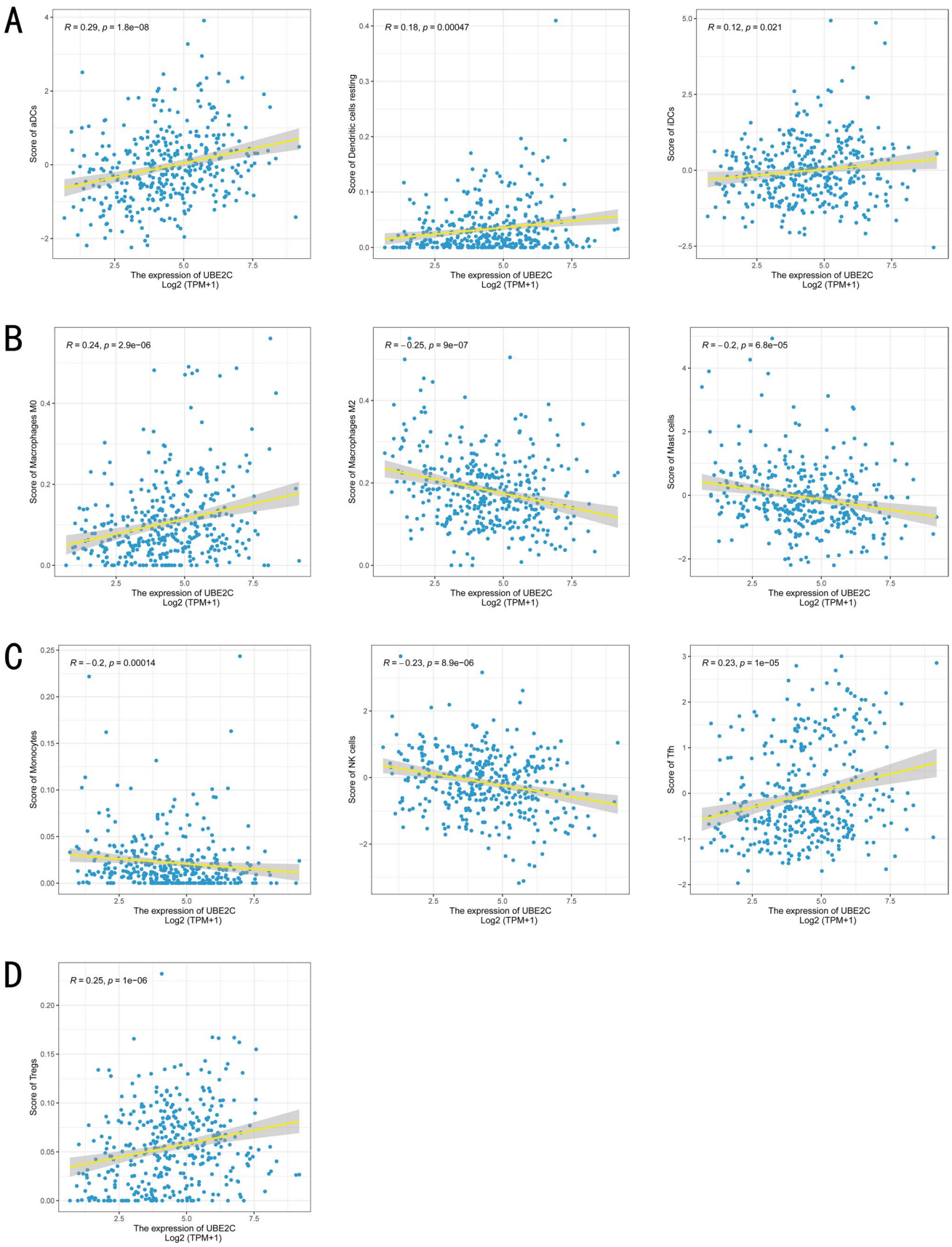

Fig. 10 Correlation between UBE2C expression and immune cell infiltration

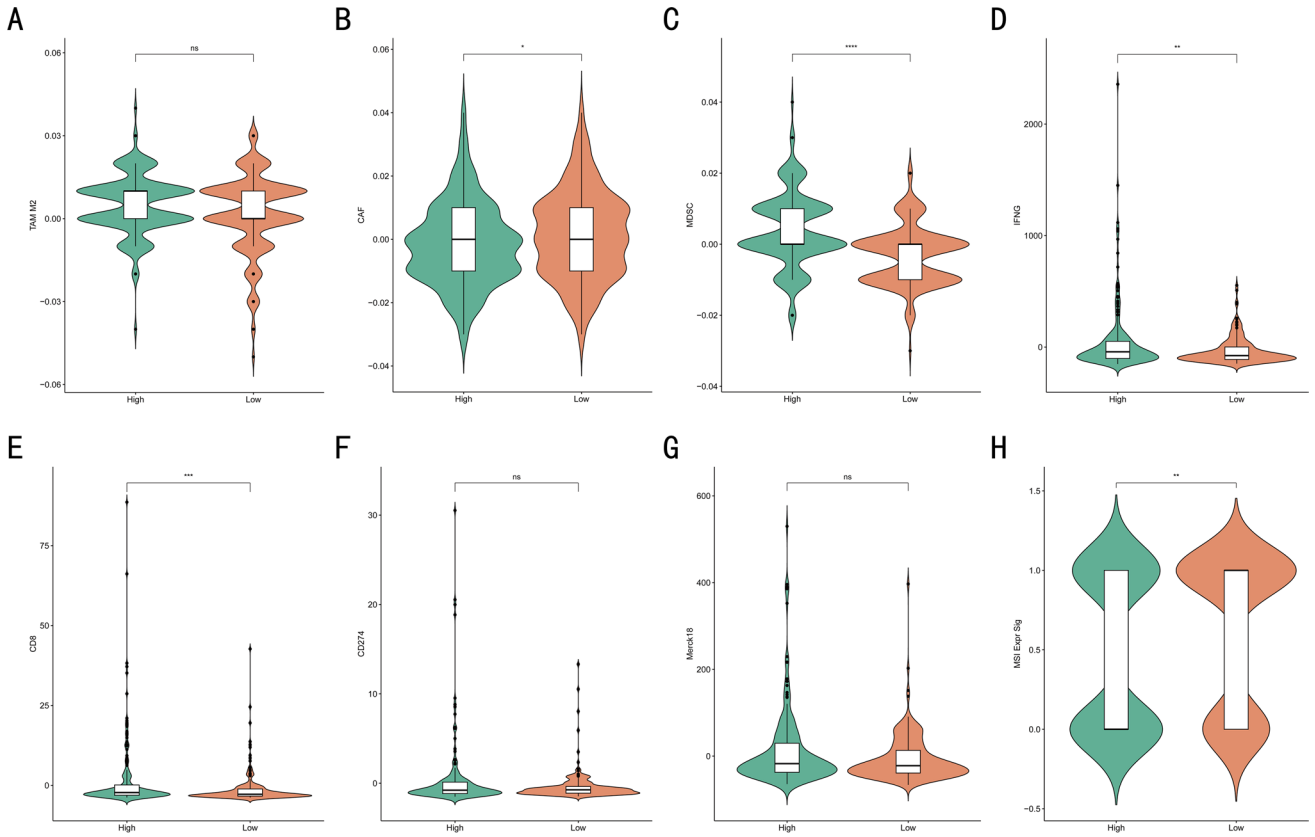

Fig. 11 Relationship between UBE2C expression and TIDE score. **A** M2 type tumor-associated macrophages (TAM M2). **B** Tumor-associated fibroblasts (CAF). **C** Myeloid-derived suppressor cells (MDSC). **D** Interferon gamma (IFNG). **E** CD8 T cells. **F** CD274. **G** Merck18. **H** Microsatellite instability (MSI). (*$p < 0.05$, **$p < 0.01$, ***$p < 0.001$, ****$p < 0.0001$, and ns, no statistical difference)

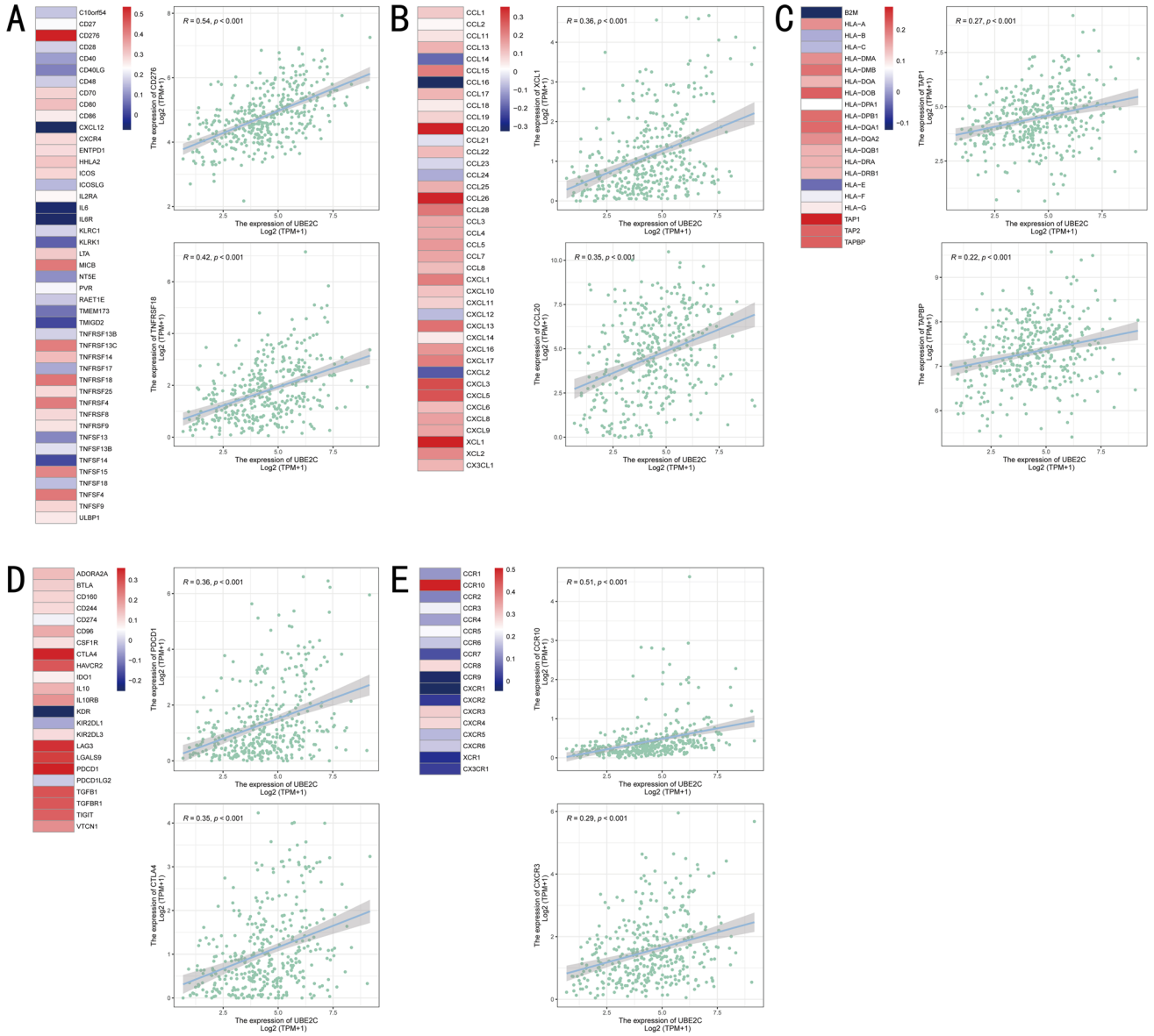

Fig. 12 Correlation between UBE2C expression and immune microenvironmental factors. **A** Immunostimulants. **B** Chemokines. **C** MHC molecules. **D** Immunosuppressive agents. **E** Chemokine receptors

Author contributions Conceptualization: Y.X., F.L.; Methodology: Y.X.; Software: Y.X., F.L., H.C.L.; Data curation: Y.X., F.L.,H.C.L.; Formal analysis: Y.X., F.L.; Visualization: Y.X., Q.B., X.Y.L.; Validation: F.L., Q.B., X.Y.L., Z.Y.W., Y.L.; Writing - original draft: Y.X., F.L., Q.B., X.Y.L., Z.Y.W., Y.L., P.F.L., L.D.; Writing—review and editing: all authors; Project administration: P.F.L., L.D., H.C.L.; Supervision: Y.X., P.F.L., L.D., H.C.L.; All authors read and approved the final manuscript.

Funding This study was supported by the President's Fund of Tarim University (TDZKSS202206).

Data availability The datasets analyzed in the study are available from the following databases: TCGA (https://portal.gdc.cancer.gov/), GTEx (https://gtexportal.org/home/), GSE121248 (https://www.ncbi.nlm.nih.gov/geo/query/acc.cgi?acc=GSE121248), GSE84402 (https://www.ncbi.nlm.nih.gov/geo/query/acc.cgi?acc=GSE84402), TIP (http://biocc.hrbmu.edu.cn/TIP/), TIDE (http://tide.dfci.harvard.edu/), TISIDB (http://cis.hku.hk/TISIDB/).

Declarations

Competing interests The authors declare no competing interests.

References

1. Llovet JM, Kelley RK, Villanueva A, et al. Hepatocellular carcinoma. Nat Rev Dis Prim. 2021;7:6. https://doi.org/10.1038/s41572-020-00240-3.
2. Sung H, Ferlay J, Siegel RL, et al. Global cancer statistics 2020: GLOBOCAN estimates of incidence and mortality worldwide for 36 cancers in 185 countries. CA Cancer J Clin. 2021;71:209–49. https://doi.org/10.3322/caac.21660.
3. Llovet JM, Montal R, Sia D, Finn RS. Molecular therapies and precision medicine for hepatocellular carcinoma. Nat Rev Clin Oncol. 2018;15:599–616. https://doi.org/10.1038/s41571-018-0073-4.
4. Palumbo A, Jr., Da Costa NM, De Martino M et al. UBE2C is overexpressed in ESCC tissues and its abrogation attenuates the malignant phenotype of ESCC cell lines. Oncotarget 2016; 7: 65876–87. https://doi.org/10.18632/oncotarget.11674
5. Chou CP, Huang NC, Jhuang SJ, et al. Ubiquitin-conjugating enzyme UBE2C is highly expressed in breast microcalcification lesions. PLoS One. 2014;9: e93934. https://doi.org/10.1371/journal.pone.0093934.
6. Mayer RJ. The meteoric rise of regulated intracellular proteolysis. Nat Rev Mol Cell Biol. 2000;1:145–8. https://doi.org/10.1038/35040090.
7. Chen S, Chen Y, Hu C, et al. Association of clinicopathological features with UbcH10 expression in colorectal cancer. J Cancer Res Clin Oncol. 2010;136:419–26. https://doi.org/10.1007/s00432-009-0672-7.
8. Mo CH, Gao L, Zhu XF, et al. The clinicopathological significance of UBE2C in breast cancer: a study based on immunohistochemistry, microarray and RNA-sequencing data. Cancer Cell Int. 2017;17:83. https://doi.org/10.1186/s12935-017-0455-1.
9. Zhang S, You X, Zheng Y, et al. The UBE2C/CDH1/DEPTOR axis is an oncogene and tumor suppressor cascade in lung cancer cells. J Clin Invest. 2023. https://doi.org/10.1172/jci162434.
10. Huang R, Guo L, Chen C, et al. System analysis identifies UBE2C as a novel oncogene target for adrenocortical carcinoma. PLoS One. 2023;18: e0289418. https://doi.org/10.1371/journal.pone.0289418.
11. Xiang C, Yan HC. Ubiquitin conjugating enzyme E2 C (UBE2C) may play a dual role involved in the progression of thyroid carcinoma. Cell Death Discov. 2022;8:130. https://doi.org/10.1038/s41420-022-00935-4.
12. Ieta K, Ojima E, Tanaka F, et al. Identification of overexpressed genes in hepatocellular carcinoma, with special reference to ubiquitin-conjugating enzyme E2C gene expression. Int J Cancer. 2007;121:33–8. https://doi.org/10.1002/ijc.22605.
13. Gao S, Gang J, Yu M, et al. Computational analysis for identification of early diagnostic biomarkers and prognostic biomarkers of liver cancer based on GEO and TCGA databases and studies on pathways and biological functions affecting the survival time of liver cancer. BMC Cancer. 2021;21:791. https://doi.org/10.1186/s12885-021-08520-1.
14. Li X, Ma Z, Mei L. Comprehensive analysis of UBE2C expression and its potential roles and mechanisms in hepatocellular carcinoma. Aging (Albany NY) 2023; 15: 7397–407. https://doi.org/10.18632/aging.204792
15. Xiong Y, Lu J, Fang Q, et al. UBE2C functions as a potential oncogene by enhancing cell proliferation, migration, invasion, and drug resistance in hepatocellular carcinoma cells. 2019. Biosci Rep. https://doi.org/10.1042/bsr20182384.
16. Wei Z, Liu Y, Qiao S, et al. Identification of the potential therapeutic target gene UBE2C in human hepatocellular carcinoma: an investigation based on GEO and TCGA databases. Oncol Lett. 2019;17:5409–18. https://doi.org/10.3892/ol.2019.10232.
17. Tomczak K, Czerwińska P, Wiznerowicz M. The cancer genome atlas (TCGA): an immeasurable source of knowledge. Contemp Oncol (Pozn). 2015;19:A68-77. https://doi.org/10.5114/wo.2014.47136.
18. GTEx Consortium. The GTEx Consortium atlas of genetic regulatory effects across human tissues. Science 2020; 369: 1318–30. https://doi.org/10.1126/science.aaz1776
19. Barrett T, Wilhite SE, Ledoux P, et al. NCBI GEO: archive for functional genomics data sets–update. Nucl Acids Res. 2013;41:D991-995. https://doi.org/10.1093/nar/gks1193.
20. Wang SM, Ooi LL, Hui KM. Identification and validation of a novel gene signature associated with the recurrence of human hepatocellular carcinoma. Clin Cancer Res. 2007;13:6275–83. https://doi.org/10.1158/1078-0432.Ccr-06-2236.
21. Wang H, Huo X, Yang XR, et al. STAT3-mediated upregulation of lncRNA HOXD-AS1 as a ceRNA facilitates liver cancer metastasis by regulating SOX4. Mol Cancer. 2017;16:136. https://doi.org/10.1186/s12943-017-0680-1.
22. Uhlén M, Fagerberg L, Hallström BM et al. Proteomics. Tissue-based map of the human proteome. Science 2015; 347: 1260419. https://doi.org/10.1126/science.1260419
23. Li T, Fu J, Zeng Z et al. TIMER2.0 for analysis of tumor-infiltrating immune cells. Nucleic Acids Res. 2020; 48: W509–14. https://doi.org/10.1093/nar/gkaa407
24. Szklarczyk D, Kirsch R, Koutrouli M, et al. The STRING database in 2023: protein-protein association networks and functional enrichment analyses for any sequenced genome of interest. Nucl Acids Res. 2023;51:D638-d646. https://doi.org/10.1093/nar/gkac1000.
25. von Mering C, Huynen M, Jaeggi D, et al. STRING: a database of predicted functional associations between proteins. Nucl Acids Res. 2003;31:258–61. https://doi.org/10.1093/nar/gkg034.
26. Xu L, Deng C, Pang B, et al. TIP: a web server for resolving tumor immunophenotype profiling. cancer Res. 2018;78:6575–80. https://doi.org/10.1158/0008-5472.Can-18-0689.

27. He Y, Jiang Z, Chen C, Wang X. Classification of triple-negative breast cancers based on immunogenomic profiling. J Exp Clin Cancer Res. 2018;37:327. https://doi.org/10.1186/s13046-018-1002-1.
28. Jiang P, Gu S, Pan D, et al. Signatures of T cell dysfunction and exclusion predict cancer immunotherapy response. Nat Med. 2018;24:1550–8. https://doi.org/10.1038/s41591-018-0136-1.
29. Ru B, Wong CN, Tong Y, et al. TISIDB: an integrated repository portal for tumor-immune system interactions. Bioinformatics. 2019;35:4200–2. https://doi.org/10.1093/bioinformatics/btz210.
30. Soerjomataram I, Bray F. Planning for tomorrow: global cancer incidence and the role of prevention 2020–2070. Nat Rev Clin Oncol. 2021;18:663–72. https://doi.org/10.1038/s41571-021-00514-z.
31. Vander Heiden MG, DeBerardinis RJ. Understanding the Intersections between Metabolism and Cancer Biology. Cell. 2017;168:657–69. https://doi.org/10.1016/j.cell.2016.12.039.
32. Pavlova NN, Zhu J, Thompson CB. The hallmarks of cancer metabolism: still emerging. Cell Metab. 2022;34:355–77. https://doi.org/10.1016/j.cmet.2022.01.007.
33. Yuan L, Yang Z, Zhao J, et al. Pan-cancer bioinformatics analysis of gene UBE2C. Front Genet. 2022;13: 893358. https://doi.org/10.3389/fgene.2022.893358.
34. Li L, Li X, Wang W, et al. UBE2C is involved in the functions of ECRG4 on esophageal squamous cell carcinoma. Biomed Pharmacother. 2018;98:201–6. https://doi.org/10.1016/j.biopha.2017.12.066.
35. Guo J, Wu Y, Du J, et al. Deregulation of UBE2C-mediated autophagy repression aggravates NSCLC progression. Oncogenesis. 2018;7:49. https://doi.org/10.1038/s41389-018-0054-6.
36. Zhang Y, Tian S, Li X, et al. UBE2C promotes rectal carcinoma via miR-381. Cancer Biol Ther. 2018;19:230–8. https://doi.org/10.1080/15384047.2017.1416939.
37. Wang R, Song Y, Liu X, et al. UBE2C induces EMT through Wnt/β-catenin and PI3K/Akt signaling pathways by regulating phosphorylation levels of Aurora-A. Int J Oncol. 2017;50:1116–26. https://doi.org/10.3892/ijo.2017.3880.
38. Wu X, Long X, Ma C, et al. Overexpression of ubiquitin-conjugating enzyme E2C is associated with worsened prognosis in prostate cancer. Int J Mol Sci. 2022. https://doi.org/10.3390/ijms232213873.
39. Yu D, Liu S, Chen Y, Yang L. Integrative bioinformatics analysis reveals CHEK1 and UBE2C as luminal a breast cancer subtype biomarkers. Front Genet. 2022;13: 944259. https://doi.org/10.3389/fgene.2022.944259.
40. Xie C, Powell C, Yao M, et al. Ubiquitin-conjugating enzyme E2C: a potential cancer biomarker. Int J Biochem Cell Biol. 2014;47:113–7. https://doi.org/10.1016/j.biocel.2013.11.023.
41. Dastsooz H, Cereda M, Donna D, Oliviero S. A Comprehensive Bioinformatics Analysis of UBE2C in Cancers. Int J Mol Sci. 2019; 20. https://doi.org/10.3390/ijms20092228
42. Malumbres M, Barbacid M. Mammalian cyclin-dependent kinases. Trends Biochem Sci. 2005;30:630–41. https://doi.org/10.1016/j.tibs.2005.09.005.
43. Zou Y, Ruan S, Jin L et al. CDK1, CCNB1, and CCNB2 are Prognostic Biomarkers and Correlated with Immune Infiltration in Hepatocellular Carcinoma. Med Sci Monit. 2020; 26: e925289. https://doi.org/10.12659/msm.925289
44. Gavet O, Pines J. Progressive activation of CyclinB1-Cdk1 coordinates entry to mitosis. Dev Cell. 2010;18:533–43. https://doi.org/10.1016/j.devcel.2010.02.013.
45. Zhao J, Yu SZ, Cai Q, et al. Identifying the key genes in mouse liver regeneration after partial hepatectomy by bioinformatics analysis and in vitro/vivo experiments. Front Genet. 2021;12: 670706. https://doi.org/10.3389/fgene.2021.670706.
46. Asghar U, Witkiewicz AK, Turner NC, Knudsen ES. The history and future of targeting cyclin-dependent kinases in cancer therapy. Nat Rev Drug Discov. 2015;14:130–46. https://doi.org/10.1038/nrd4504.
47. Hochegger H, Takeda S, Hunt T. Cyclin-dependent kinases and cell-cycle transitions: Does one fit all? Nat Rev Mol Cell Biol. 2008;9:910–6. https://doi.org/10.1038/nrm2510.
48. Ng, Il, Zhang J, Tian T et al. Network-based screening identifies sitagliptin as an antitumor drug targeting dendritic cells. J Immunother Cancer. 2024; 12. https://doi.org/10.1136/jitc-2023-008254
49. Finotello F, Trajanoski Z. New strategies for cancer immunotherapy: targeting regulatory T cells. Genome Med. 2017;9:10. https://doi.org/10.1186/s13073-017-0402-8.
50. Currie AJ, Prosser A, McDonnell A, et al. Dual control of antitumor CD8 T cells through the programmed death-1/programmed death-ligand 1 pathway and immunosuppressive CD4 T cells: regulation and counterregulation. J Immunol. 2009;183:7898–908. https://doi.org/10.4049/jimmunol.0901060.
51. Rowshanravan B, Halliday N, Sansom DM. CTLA-4: a moving target in immunotherapy. Blood. 2018;131:58–67. https://doi.org/10.1182/blood-2017-06-741033.
52. Huang GZ, Chen ZQ, Wu J, et al. Pan-cancer analyses of the tumor microenvironment reveal that ubiquitin-conjugating enzyme E2C might be a potential immunotherapy target. J Immunol Res. 2021;2021:9250207. https://doi.org/10.1155/2021/9250207.
53. Cai D, Tian F, Wu M, et al. UBE2C is a diagnosis and therapeutic biomarker involved in immune infiltration of cancers including lung adenocarcinoma. J Cancer. 2024;15:1701–17. https://doi.org/10.7150/jca.92473.
54. Fu Y, Liu S, Zeng S, Shen H. From bench to bed: the tumor immune microenvironment and current immunotherapeutic strategies for hepatocellular carcinoma. J Exp Clin Cancer Res. 2019;38:396. https://doi.org/10.1186/s13046-019-1396-4.
55. Hinshaw DC, Shevde LA. The tumor microenvironment innately modulates cancer progression. Cancer Res. 2019;79:4557–66. https://doi.org/10.1158/0008-5472.Can-18-3962.
56. Noy R, Pollard JW. Tumor-associated macrophages: from mechanisms to therapy. Immunity. 2014;41:49–61. https://doi.org/10.1016/j.immuni.2014.06.010.
57. Song W, Shen L, Wang Y, et al. Synergistic and low adverse effect cancer immunotherapy by immunogenic chemotherapy and locally expressed PD-L1 trap. Nat Commun. 2018;9:2237. https://doi.org/10.1038/s41467-018-04605-x.